

Novel injection molding technique for coating soft-siloxanes on neural microelectrodes

for stable pO<sub>2</sub> sensing using MR imaging

by

Livia de Mesquita Teixeira

A thesis presented in Partial Fulfillment  
of the Requirements for the Degree of  
Master of Science

Approved November 2018 by the  
Graduate Supervisory Committee:

Jitendran Muthuswamy, Co-Chair

Vikram Kodibagkar, Co-Chair

Arati Sridharan

ARIZONA STATE UNIVERSITY

December 2018

## ABSTRACT

There is a critical need for creating an implantable microscale neural interface that can chronically monitor neural activity and oxygenation. These are key aspects for understating the development of impaired neural circuits and their functions. A technology with such capability would foster new insights in the studies of brain diseases and disorders. The propose is that MR-PISTOL (Proton imaging of Siloxane to Map Tissue Oxygenation Levels) imaging technique can be used for direct measurements of oxygen partial pressure at microelectrode-tissue interface. The strategy consists of coating microelectrodes with soft-silicone, a ultra-soft conductive PDMS (polydimethylsiloxane), as a carrier for liquid siloxanes MR-PISTOL contrast agents. This work presents a proof-of-concept of an injection molding technique for batch fabricate microelectrodes with such coating. Also, reports stability studies of soft-silicone loaded with liquid polydimethylsiloxane (PDMSO) in rodent brains. A batch of thirty coated carbon electrodes was achieved using candy molds. Coating uniformity was evaluated in twelve probes. They were randomly chosen and imaged with a custom image setup that allows 90° rotation of the probes. The total average coating thickness before and after rotation were 0.397 millimeters with standard deviation of 0.070 millimeters and 0.442 millimeters with standard deviation of 0.062 millimeters. Therefore, data confirms that this technique yields uniform coating. Stability of fabricated coated carbon electrodes unloaded (n= 3) and loaded with PDMSO (n= 3) was assessed. 3D X-ray imaging using Zeiss Xradia 520 machine was chosen for studying coatings mechanical stability in ex-vivo rat brain. Transmission electron microscopy (TEM) and scanning

electron microscope (SEM) with an energy dispersive x-ray microanalysis (EDS) detector were used to investigate their chemical stability in *in vivo* mouse brain. Initial EDS analysis from TEM and SEM of acute (6 hours) and chronic (2 weeks) brain slices suggest that PDMSO does not leach into brain. More experiments should be done to confirm and endorse this finding. The mechanical study shows that coating loaded with PDMSO delaminated during insertion. This was not observed with electrodes used in the chemical stability studies. Further experiments need to be done to identify possible causes of mechanical failures.

To my parents Antonio Bernardo and Luzenilde, sister Lais and friends in special Eric. I cannot describe in words how their love and support helped me during this endeavor.

Thank you.

## ACKNOWLEDGEMENTS

I would like to thank the members of my thesis committee Dr. Jitendran Muthuswam, Dr. Vikram Kodibagkar and Arati Sridharan for their mentorship. David Lowry for helping with TEM and SEM biological sample preparation from the Life Science Electron Microscopy, Eyring Materials Center, ASU. Karl Weiss and Ken Mossman for helping with TEM, SEM imaging and EDS analyzes from the John M. Cowley Center for High Resolution Electron Microscopy (CHREM, ASU). Also, Jason Williams from Nik Chawla's group for his assistance with the 3D X-ray imaging of the samples. Moreover, we would like to thank the Ira A. Fulton Schools of Engineering for partially funding this work through the Master's Opportunity for Research in Engineering (MORE) program.

# TABLE OF CONTENTS

	Page
LIST OF FIGURES.....	ix
CHAPTER	
1. INTRODUCTION.....	1
2. BATCH FABRICABLE PROCESS FOR COATING ELECTRODES WITH SOFT-SILICONE.....	4
Overview.....	4
POLYMER COATING TECHNIQUES FOR NEURAL INTERFACES.....	6
Electropolymerization.....	6
Spin-Coating.....	7
Dip-Coating.....	8
Chemical Vapor Deposition.....	9
Electrospinning.....	10
Molding Technique.....	11
INDUSTRIAL POLYMER MANUFACTURING PROCESS.....	12
Injection Molding background.....	12

CHAPTER	Page
INJECTION MOLDING FOR COATING MICROELECTRODES WITH SOFT-SILICONE.....	14
MATERIALS AND METHODS.....	14
Fabrication of Carbon Microelectrodes.....	14
Preparation of Soft-Silicone for Coating Application.....	15
Preparation of hard-PDMS for hard-PDMS mold fabrication.....	15
Preparation of Candy Material for Super Soft Lithography.....	15
Design and Manufacturing of Candy Molds.....	16
Carbon Microelectrodes Array Assembly for Coating Injection Molding.....	17
Injection Molding Process.....	18
Setup for Imaging Soft-Silicone Coatings and Analysis.....	19
RESULTS.....	20
Candy Molds .....	20
Soft-Silicone Coated Carbon Microelectrodes.....	21
Discussion.....	22
Conclusions and Future Work.....	23

CHAPTER	Page
3. STABILITY STUDIES OF SOFT-SILICONE LOADED WITH PDMSO.....	24
Outline.....	24
MATERIALS AND METHODS.....	25
Preparation of Soft-Silicone Coated Carbon Microelectrodes for Animal Experiments.....	25
Preparation of artificial cerebrospinal fluid.....	25
SURGERY PROCEDURES FOR ACUTE ANIMAL EXPERIMENTS.....	26
Transmission Electron Microscopy (TEM) and Scanning Electron Microscope (SEM) with Energy Dispersive X-ray Analyzes (EDS).....	26
3D X-ray imaging.....	27
Surgery Procedure for Scanning Electron Microscope (SEM) with Energy Dispersive X-ray Analysis (SEM/EDS) Chronic Animal Experiment.....	27
ENERGY DISPERSIVE X-RAY ANALYZES.....	27
Background.....	28
Criterion for Brain Tissues Silicone Analysis .....	28
RESULTS.....	29
ANALYSIS OF BRAIN SLICES.....	29



CHAPTER	Page
TEM/EDS Analysis of Acute Animal Experiment.....	29
SEM/EDS Analysis of Acute Animal Experiment.....	31
SEM/EDS Analysis of Chronic Animal Experiment.....	33
Study of Mechanical Integrity of Control and Sample Coated Carbon Microelectrodes in Ex-Vivo Rat Brain.....	35
Discussion.....	36
Conclusion and Future Work.....	38
REFERENCES.....	40
APPENDIX.....	43
A SUPPLEMENTAL MATERIAL FOR CHAPTER III.....	43
TEM AND SEM SAMPLE PREPARATION PROTOCOLS.....	44
TEM/EDS ANALYSIS OF ACUTE ANIMAL EXPERIMENT.....	46

## LIST OF FIGURES

Figure	Page
<p>1 An example of platinum microelectrodes coated (black color) and non-coated (light color) with PEDOT/pTS by electrochemical polymerization from Green <i>et al.</i> 2015 [10].....</p>	7
<p>2 Examples of neural interfaces that utilized spin-coating method during fabrication process. a) PDMS-based integrated stretchable MEA adapted from Guo <i>et al.</i> 2013 [14]. b) a mesh intracortical electrode made by patterning photosensitive-polyimide (PSPI) from Kato <i>et al.</i> 2012[15].....</p>	8
<p>3 Schematic that shows dip coating of a Michigan neural probe with 1 wt% sodium alginate solution and crosslinked with 0.5 M CaCl<sub>2</sub>, from Kim <i>et al.</i> 2010 [16].....</p>	9
<p>4 Schematic of coating neural microelectrodes with parylene via chemical vapor deposition. Carbon microelectrode array a) before and b) after parylene deposition (yellow trace). From Schwerdt <i>et al.</i> 2018.....</p>	10
<p>5 Example of Michigan probe coated with anti-inflammatory drug (dexamethasone) incorporated by electrospinning from Abidian <i>et al.</i> 2009.....</p>	11
<p>6 A schematic of an injection molding machine for liquid silicone rubber. Adapted from [24].....</p>	13
<p>7 Overview of the steps to fabricate candy molds. a) 3D printed master mold; b) soft lithography to fabricate hard-PDMS mold; c) hard-PDMS mold; d) super soft lithography to fabricate candy mold; e) Candy mold.....</p>	17

Figure	Page
8 CAD model of carbon microelectrodes array used for the injection molding process...	18
9 Shows the apparatus utilized for filling the candy molds with soft-Silicone. 1) Syringe filled with soft-Silicone; 2) Micromanipulator; 3) Nitrogen compressed gas cylinder; 4) Ultimius I Fluid dispensing system (EFD); 5) Movable platform.....	19
10 Custom-build image setup to image coated carbon electrodes.....	20
11 Shows the fidelity of pattern transferring using super soft lithography. From left to right, ABS master mold, hard-PDMS mold and candy mold.....	20
12. Displays samples of carbon electrodes coated with soft-silicone before (left) and after (right) 90 degrees of rotation. a) electrode 1, b) electrode 2 and c) electrode 3.....	21
13. Graphs of coating thickness of 10 electrodes before (a) and after (b) 90 degrees of rotation.....	22
14 a) TEM imaging of a random region of the control brain tissue. b) EDS spectrum from sampling point 1. A well-defined peak of silicon was not detected. But osmium peak was, and it was greater than 400 counts.....	30
15 Shows in (a) the SEM image of the sample brain tissue done at 15.0 keV and 61x magnified. The electrode puncture is located at the top left (see black arrow) b) the EDS mapping of silicon.....	32
Displays the EDS spectrum of the whole sample brain tissue and the EDS analyses done by the SEM software.....	32

Figure	Page
17 a) SEM imaging at 5 keV of the sample brain tissue puncture 200x magnified. b) EDS mapping of silicon and carbon. c) EDS spectrum of the brain tissue surrounding the puncture.....	33
18 a) SEM imaging with magnification of 130x at 15 kV showing the electrode track of control brain tissue. b) the EDS spectrum of the control brain tissue.....	34
19 a) SEM imaging with magnification of 220x at 15 kV exposing the electrode track sample brain tissue. b) the EDS spectrum of the sample brain tissue.....	35
20 3D x-ray of coated carbon microelectrodes implanted in the cerebral cortex of the rat brain. Coated carbon fiber unloaded with PDMSO is seen under the black arrow on left and the coated carbon fiber loaded with PDMSO is seen under the black arrow on the right.....	36

## CHAPTER 1

### INTRODUCTION

The nervous system is the utmost part of the body. It governs vital mechanisms such as body movement, breathing, heart rate, thinking, feelings, sensations, memories and consciousness. Its building block, neurons, are responsible for generating, transmitting and interpreting the information that execute and control such mechanisms. Injury, aging, neurological diseases and disorders negatively alter their function.

Depending on the severity and location of affected neurons, health problems that are life-threatening or reduce quality of life can appear. For this reason, the comprehension of normal and pathological neurons is decisive for the development of prevention and therapies, upholding the health and welfare of humankind. In recent years, the neural engineering community has been developing neurotechnologies as an effort to accomplish this goal.

Implantable microscale neural interface is the current neurotechnology that enables the study of neural circuits and individual neurons at cellular resolution. Although this technology is immensely contributing for advances of neuroscience knowledge and, also, revolutionizing the treatment of injury, diseases and disorders of the nervous system, it does not provide other essential information. Current devices do not monitor factors that regulate neuronal activity. For example, local oxygen partial pressure ( $pO_2$ ) in the nervous tissue, which represents the equilibrium between oxygen delivery and its consumptions, dictates the activity and function of neurons and their supportive cells, glial cells.

Consequently, if an implantable neural interface could quantitatively chronically assess  $pO_2$  levels, it would greatly contribute to the understanding of underlying metabolic changes in the tissue that originate and maintain the recorded neural activity. This knowledge would further facilitate the investigation of dysfunctional neural circuits that arise in aging, neurological diseases and disorders and injury. Hence, contributing to their prevention and treatment.

A variety of techniques can be used to determine the oxygenation of a biological tissue [1]–[8]. Among them, the Proton Imaging of Siloxanes to Map Tissue Oxygenation Levels (MR-PISTOL) imaging technique developed by Kodibagkar *et al.* 2008 [9]. It drawn attention as a candidate technique to be merged with implantable microscale neural interface because it provides quantitative, microscale spatial mapping of  $pO_2$ . Besides, it has potential to be used in conjecture with other MRI imaging methods, such as BOLD-fMRI, making possible to study the relationship between micro vasculature and measured nervous tissue  $pO_2$  levels.

The current approach that is being explored to incorporate siloxanes MR-PISTOL contrast agents into neural interfaces is to coat the microelectrodes with a novel soft-silicone material that can hold them.

The contributions of this work are towards the development of a process that can successfully coat microelectrodes arrays simultaneously with the soft-silicone. Furthermore, to survey methods to assess soft-silicone stability in nervous tissue when it is loaded with liquid polydimethylsiloxane MR-PISTOL contrast agent (PDMSO).

Accordingly, chapter 2 demonstrates the method that batch fabricates coated microelectrodes with the soft-silicone material. The introduction briefly overviews soft

coatings, specifically, the soft-silicone. Next, polymer coating techniques for neural interfaces and the industry polymer injection manufacturing process, that inspired the design of developed fabrication, are described. Last, the developed injection molding is described, and its results are discussed.

Chapter 3 reports the studies that investigated the stability of fabricated coated microelectrodes loaded with PDMSO in the brain of rodents. The rationale behind mechanical and stability tests and methods chosen to assess them are first shown, followed by, the experimental description of the acute and chronic experiments. The results of surveyed methods, 3D X-ray imaging for mechanical stability study, Transmission electron microscopy (TEM) and scanning electron microscope (SEM) with an energy dispersive x-ray microanalysis (EDS) detector for chemical stability studies, are then presented and evaluated.

## CHAPTER 2

### BATCH-FABRICABLE PROCESS FOR COATING MICROELECTRODES WITH SOFT-SILICONE

#### Overview

The development of soft coatings for neural probes emerged from the need to improve current neural probe technology. Although conventional metal-based microelectrodes arrays have been used for decades, it is thought that they reached a plateau [10]. The main hypothesis is that characteristics of the metal, such as stiffness, inertness and surface morphology, does not promote effective interaction with the surrounding nerve tissue. In fact, chronic foreign body response is commonly observed in nerve tissue subjected to metal microelectrode implantation. This body response is seen as the limiting-factor to achieve long-term stable performance.

A variety of strategies have been pursued to reduce chronic foreign body response. Soft coating is a strategy that focuses on reducing mechanical mismatch between stiff neural probes and surrounding tissue. Many materials are being explored for the fabrication of soft coating such as conductive polymers, carbon nanotubes, hydrogels, conductive hydrogel, bioactive coatings and others. The soft-silicone developed by Sridharan *et al.*[11] is an example. The coating is a conductive polymer made by an elastomer matrix, polydimethylsiloxane (PDMS), doped with carbon nanotubes. This material is designed to match the elastic modulus (~5-8 kPa) and viscoelastic properties of cortical brain. The group demonstrated that this coating is a promising solution for correcting mechanical mismatch between brain and neural probes,



while promoting electrical coupling. In the study, platinum-iridium electrodes that were dip-coated with this composite material exhibited stable Nyquist plots over one year.

In addition to mechanical amelioration, soft-silicone coating has attractive characteristics for other applications. Beauchamp [12] proved the feasibility of using it as a host matrix for PDMSO. Quantitative measurements of  $pO_2$  within soft-silicone coating applied on catheter tubes implanted in ex-vivo mouse brain was accomplished. Likewise, a recent study in the lab demonstrated the practicability of using same approach for measuring  $pO_2$  levels around chronic implanted coated carbon electrode in *in vivo* mouse brain. The coating was able to provide stable  $pO_2$  measurements for at least a month.

Due to these exemplary results, we are working to further develop this technology. The next steps will be to test MRI-PISTOL technique in carbon microelectrode array coated with the soft-silicone. However, current coating application is not scalable. The process is done by manually coating each carbon electrode individually. The pre-polymer is applied on the carbon fiber with the assistance of a needle and it is placed on a hot plate to cure. To achieve uniform coating, which is desired for obtaining a uniform  $pO_2$  spatial map around the microelectrode, the soft-silicone is manipulated with the needle to ‘spread’ out on the surface of the electrode. If this step is not done, the resulting coating is non-uniform because soft-silicone tends to spontaneously form as blobs after curing due to surface tension. Therefore, a batch fabrication process that yields uniform soft-silicone coating on carbon microelectrodes is needed.

## POLYMER COATING TECHNIQUES FOR NEURAL INTERFACES

### Electropolymerization

Electrochemical polymerization is a method for coating metallic electrodes with a thin layer of a conductive polymer. Examples of conductive polymers used for neural probes are poly(3,4-ethylene dioxythiophene) (PEDOT), polythiophene (PTh), poly(aniline) (PANI), poly(aniline) (PANI) [10]. These polymers present a highly conjugated electronic structure that allows charge transport along the backbone of the polymer chain. Their conductivity can be enhanced through a doping process, a similar strategy of that used in semiconductors doping process [13]. Many external stimuli (e.g, ultraviolet light, chemical, voltage/current and magnetic field) can be used to favor the polymerization and choice depends on initial monomer. Voltage/current is typically used for coating microelectrodes of neural probes. The process consists of immersing the microelectrodes in a monomer solution and applying a voltage between the solution and microelectrodes desired to be coated. This results in the growth of conductive polymer layer on the surface of selected microelectrodes (see figure 1). Many factors influence the electrical and physical properties of the conductive polymers such as applied voltage/current, dopant choice, temperature, pH of monomer solution and others.

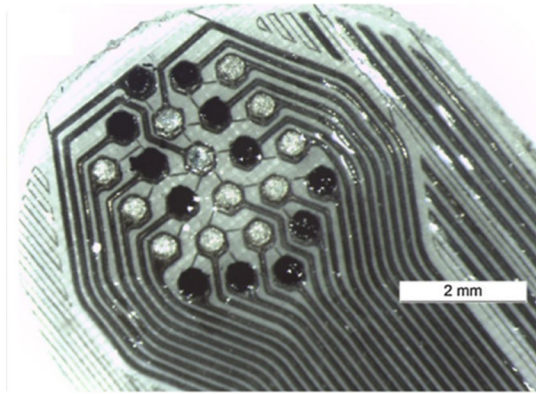


Figure 1 An example of platinum microelectrodes coated (black color) and non-coated (light color) with PEDOT/pTS by electrochemical polymerization from Green *et al.* 2015 [10].

### Spin-Coating

Spin-Coating is one of the many methods for creating uniform thin polymer films, specifically for coating flat substrates. The technique is done under a spin-coater machine. The substrate is placed in the machine with a small amount of the prepolymer on the surface. Then, substrate is rotated to spread the polymer on its entire surface. Subsequently, it is placed on a hot plate to cure the pre-polymer film. The thickness of the resulted film depends on the angular speed of spinning, viscosity, solvent and concentration of the solution. Examples of polymers are polydimethylsiloxane (PDMS), polyimide and SU-8 photoresist (epoxy-based negative photoresist). This process is often used to create planar microelectrodes arrays (see figure 2).

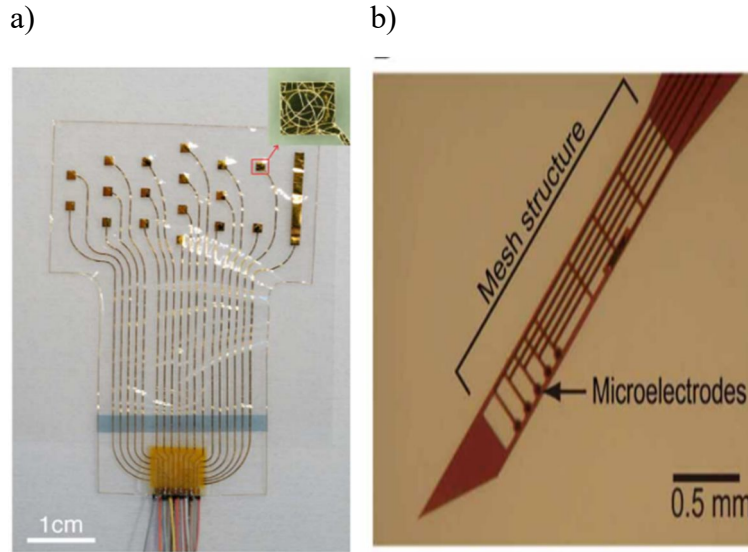


Figure 2 Examples of neural interfaces that utilized spin-coating method during fabrication process. a) PDMS-based integrated stretchable MEA adapted from Guo *et al.* 2013 [14]. b) a mesh intracortical electrode made by patterning photosensitive-polyimide (PSPI) from Kato *et al.* 2012[15].

### Dip-Coating

In dip-coating, three steps need to be followed to coat neural probes. First step is the immersion of the probe at a constant speed in a polymer solution. Then, the probe stays for a certain time in the solution and is pulled up. During the pulling process, the polymer deposits itself on the surface while the solvent evaporates to form a thin layer throughout the probe. The withdrawing speed determines the thickness of the coating, for example, fast withdrawal results in thicker coating. Other factors that cause the resulted thin film are submersion time, solution composition, concentration, number of solutions in each dipping sequence, number of dipping cycles and environment humidity. An example of a dipping coating process of a neural probe can be seen in figure 3.

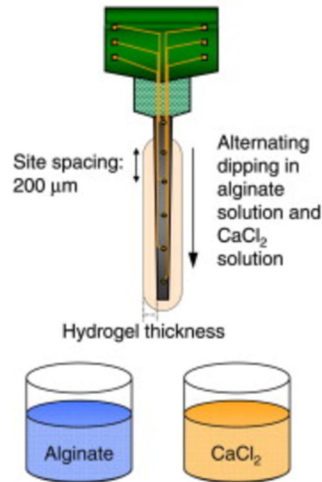


Figure 3 Schematic that shows dip coating of a Michigan neural probe with 1 wt% sodium alginate solution and crosslinked with 0.5 M  $\text{CaCl}_2$ , from Kim *et al.* 2010 [16].

### Chemical Vapor Deposition

Chemical vapor deposition is a free-solvent coating method. There are a variety of chemical vapor deposition methods. The process that will be described is for the deposition of Parylene, a common polymer for insulating Food and Drug Administration (FDA) approved implants [17] (see figure 4). The process involves three main stages: sublimation, pyrolysis, and polymerization. Before the start of the process, electrodes need to be coated with an adhesion promoter to endorse deposition of the polymer throughout the surface to be coated. The chemical vapor deposition process happens under a vacuum deposition chamber. The first step is the sublimation step where the polymer dimmers are loaded and heated until vaporized. The vaporized dimers flow to the pyrolysis furnace. In this step a thermochemical treatment called pyrolysis takes place. The polymer dimmers are split into monomers to form a monomer vapor. This monomer vapor leaves the pyrolysis furnace and enters the deposition chamber that is at

room temperature. The last phase, polymerization, happens in the deposition chamber. The monomer vapor bond to the surface, forming a polymer layer.

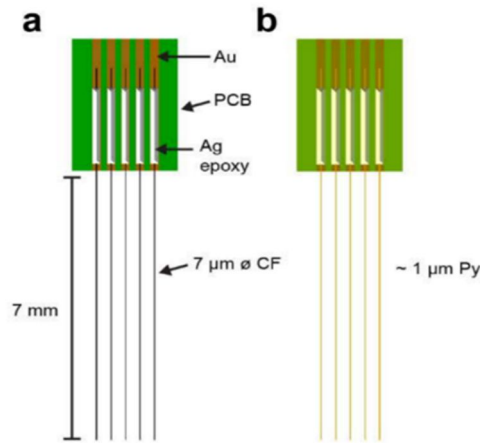


Figure 4 Schematic of coating neural microelectrodes with parylene via chemical vapor deposition. Carbon microelectrode array a) before and b) after parylene deposition (yellow trace). From Schwerdt *et al.* 2018.

## Electrospinning

Electrospinning is a technique to fabricate ultrafine polymer fibers (nm to microns) using electrostatic force. The general setup utilizes a syringe, containing the polymer solution, collector, where fibers will be deposited, and high-power voltage source, to create an electric field between the syringe and collector. The process initiates when the electric field induce charge accumulation at the liquid surface to generate an electrostatic repulsion higher than the surface tension of the liquid. This results in a deformation of the polymer solution at the tip of the syringe known as Taylor cone. The charged polymer solution is ejected from the Taylor Cone towards the collector. Ultrafine polymer fibers are deposited on the collector as the solvent evaporates during flight motion. An example of using electrospinning for coating neural probes can be seen in figure 5.

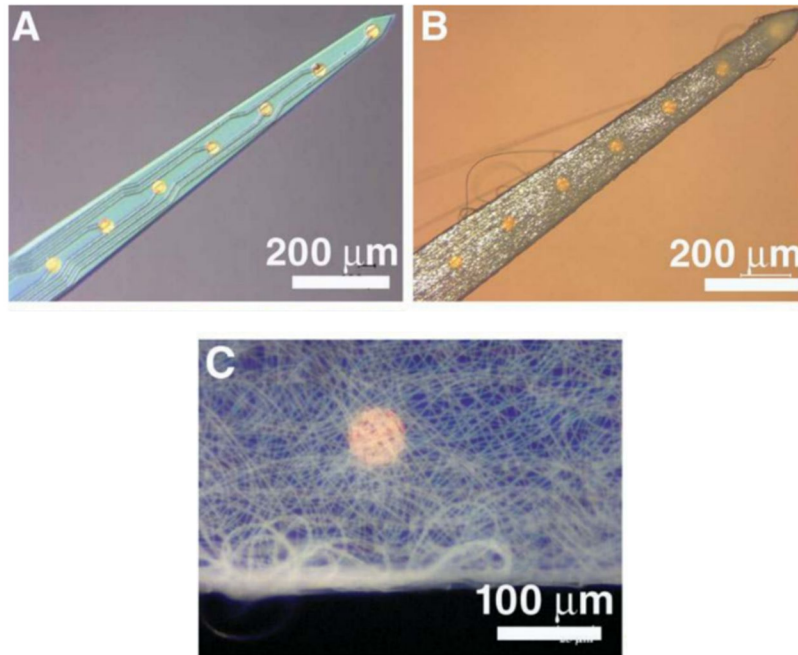


Figure 5 Example of Michigan probe coated with anti-inflammatory drug (dexamethasone) incorporated by electrospinning from Abidian *et al.* 2009.

### Molding Technique

Molding technique is another strategy explored for coating microelectrodes. In brief, it utilizes mold to shape the polymer coating on the neural probe. As an example, Trikantopoulos *et al.*[20], investigated the usage of 3D-printed mold to batch fabricate carbon-fiber microelectrodes for measuring electro-active neurotransmitters *in vivo*. They were able to fabricate 40 microelectrodes simultaneously. Carbon electrodes were individually inserted in a stainless-steel cannula needle. Each cannula needle was placed in one of the 40 channels of a 3D-printed acrylonitrile butadiene styrene (ABS) mold. Then, polyimide resin was poured in each channel and allowed to cure. The removal of the carbon microelectrodes was done by manually bending the 3-D molds and using tweezers to pull out the coated microelectrodes. Another example is from Lo *et al.*[21]. The group developed a proof-of-concept fabrication process for coating small flexible

neural probes with a biodegradable polymer (tyrosine-derived-polycarbonate (E5005(2K) polymer). Their idea was to coat low stiff probes with a temporary stiffer biodegradable material to aid their insertion into neural tissue. PDMS was used as mold for coating a non-functional miniaturized SU-8 probe with the biodegradable polymer. The group choose PDMS because it has weak adhesion with SU-8, favoring mechanical lift-off demolding. Also, to avoid wet chemical etching of sacrificial layers since the polymer coating degrades in aqueous solutions.

## INDUSTRIAL POLYMER MANUFACTURING PROCESS

### Injection Molding background

Injection Molding [22] is one of the manufacturing processes existing in polymer industry to mass produce the polymer parts. Other methods are extrusion, thermoforming, compression molding, blow molding, and many others. John Wesley Hyatt and his brother Isaiah Hyatt patented the first injection molding machine in 1872. Over the years, the method was refined, and its adoption rapidly expanded during World War II because of the high demand of inexpensive mass-produced parts [23].

Generally, injection machines are custom-built according to material type and the parts desired to fabricate. However, all injection machines are composed by three main components: injection unit, mold tool and clamp unit. An example of an injection molding machine can be seen in figure 6. Succinctly, the injection unit is mainly responsible for injecting a set volume of polymer consistently and accurately to the mold cavities. The mold tool receives the injected polymer and distribute it in its cavities. The cavities patterns follow the desired part design. Then, the mold tool is either heated or



cooled down to fix the polymer shape. The temperature depends on the type of polymer. For example, if it is a thermoplastic, the thermoplastic is melted in the injection unit and is cooled down in the mold tool. If it is a thermoset polymer, such as Liquid Silicone Rubber (LSR), the mold tool is at high temperature to cure the polymer. Another component of injection molding machine is the clamp unit. The clamp unit is responsible for holding the mold tool in place during the injection process and assists with the ejection of the fabricated part.

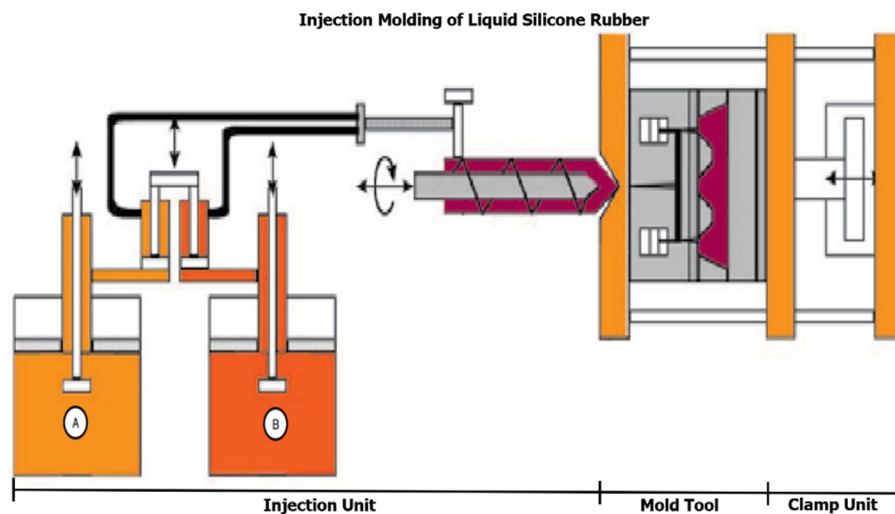


Figure 6 A schematic of an injection molding machine for liquid silicone rubber. Adapted from [24].

The injection molding process offers advantages in comparison to other industry methods as, it allows the creation of polymer parts with different designs and sizes per each fabrication cycle. Moreover, it permits the usage of multiple polymers to fabricate composite parts. Despite these positive characteristics, disadvantages exist. One of these disadvantages is the shear stresses that occurs during the process. Polymers used need to be able to withstand these mechanical stresses, so good quality parts can be created.

## INJECTION MOLDING FOR COATING MICROELECTRODES WITH SOFT-SILICONE

Injection molding was the method chosen among the described polymers methods for the development of a batch-fabricable process for coating microelectrodes with soft-silicone. The main reason is the possibility to be automatized in the future, thus making possible mass production of microelectrode arrays coated with the composite material but there are differences between proposed injection molding and industry injection molding. The major difference is the usage of water-soluble molds instead of metal molds, commonly used in injection molding, to avoid mechanical stresses during demolding. Therefore, allowing the shaping of very-soft materials. Other differences are related to the injection steps. Since the proposed fabrication is for a specific application (coating substrates), steps need to be adapted to meet the unique requirements of a coating application. A proof-of-concept fabrication process based on injection molding will be represented along with its feasibility study.

## MATERIALS AND METHODS

### Fabrication of Carbon Microelectrodes

Individual carbon fibers (~7 microns width) were clustered to create carbon microelectrodes (150-180 width) with the assistance of a glass micropipette. Carbon electrodes were taped on a glass slide with polyimide tape for the epoxy (epoxylite™) application process. Five electrodes were insulated per glass slide. The epoxy was applied manually on the surface of the carbon electrode with a needle and gently squeezed with tweezers to avoid formation of epoxy globs through the electrode length. The curing was

done by two consecutive steps. In the first step, after epoxy application, electrodes were placed on a hot plate at 105°C for about 3 minutes. The same procedure was repeated in the second step; however, the curing time was increased by 2-fold.

#### Preparation of Soft-Silicone for Coating Application

Sylgard 184 (Dow Corning) was mixed with a cross-linking ratio of 1:75 to produce soft-brain like PDMS (Elastic modulus  $\sim$  3-5 kPa). As a proof of concept, soft-silicone matrix was fabricated without carbon nanotubes to test the fabrication process. The soft-silicone was poured in a centrifuge tube to be degassed in a centrifuge (1000 rpm) for about 5 minutes. Next, it was poured into a petri dish to be further degassed in a vacuum chamber for 1 hour and 30 minutes. Afterwards, it was transferred into a syringe with a 32-gauge needle which was later attached to a fluid dispensing system (Nordson EFD Ultra 2400 Series).

#### Preparation of hard-PDMS for hard-PDMS mold fabrication

Hard-PDMS was fabricated in a similar manner described in the previous section. The only differences are the cross-linking ratio of 1:10 to fabricate PDMS (Elastic modulus  $\sim$ 1000kPa) and the storage. The mixture was left in the centrifuge tube until further usage in the fabrication of hard-PDMS mold.

#### Preparation of Candy Material for Super Soft Lithography

Sucrose and Karo light corn syrup in a 2:1 v/v ratio, as recommended in [25], were mixed in a beaker and placed on a hot plate at 220°C until color changed to medium

brown. The fabrication of candy material is done right before starting the candy-casting step in the hard-PDMS mold. Typically, 4 grams of sucrose and 2 grams of Karo light corn syrup had a yield of 10 candy molds.

### Design and Manufacturing of Candy Molds

A master mold was designed in SolidWorks software and printed in a 3D Stratasys Mojo (100 microns nozzle) machine with a layer thickness resolution of 0.17mm. 3D printed molds were made of acrylonitrile butadiene styrene (ABS). The pattern consisted of three half cylinders with a width of 0.35mm and 4mm of length separated by a pitch of 2mm.

The candy molds were manufactured with super soft lithography [25]. Overall fabrication steps are shown in figure 7. ABS model was placed in a petri dish and Hard-PDMS was poured. The petri dish was placed in a vacuum chamber for about 1 hour and 30 minutes to de-gas the hard-PDMS. Subsequently, the petri dish was placed on a hot plate at 70°C for 2 hours to cure the hard-PDMS. After curing, ABS mold was removed carefully. For the candy casting step, hard-PDMS mold is first left on a hot plate at 100 °C. This step is important to avoid large temperature differences between the candy and hard-PDMS, affecting pattern transferring.

Subsequently, right before pouring the candy, the hard-PDMS mold was placed on benchtop. Candy was poured into the patterned molds and compressed with a PDMS membrane (portion cut from hard-PDMS mold that did not contain the pattern molds) at the top. Pressure was applied manually on the PDMS membrane until the temperature of the hard PDMS decreased to room temperature. Next, water-soluble candy molds were

removed cautiously and stored in a chamber room with controllable temperature and humidity (23 °C and 12% humidity) until its usage in soft coating injection molding process.

### Assembly of Carbon Microelectrodes Array for Injection Molding

Carbon microelectrodes were setup as seen in figure 8 for the coating injection molding. The ABS 3D printed molds serve as the support for the electrodes. The carbon fibers are placed in the microchannels and taped down with polyimide tape.

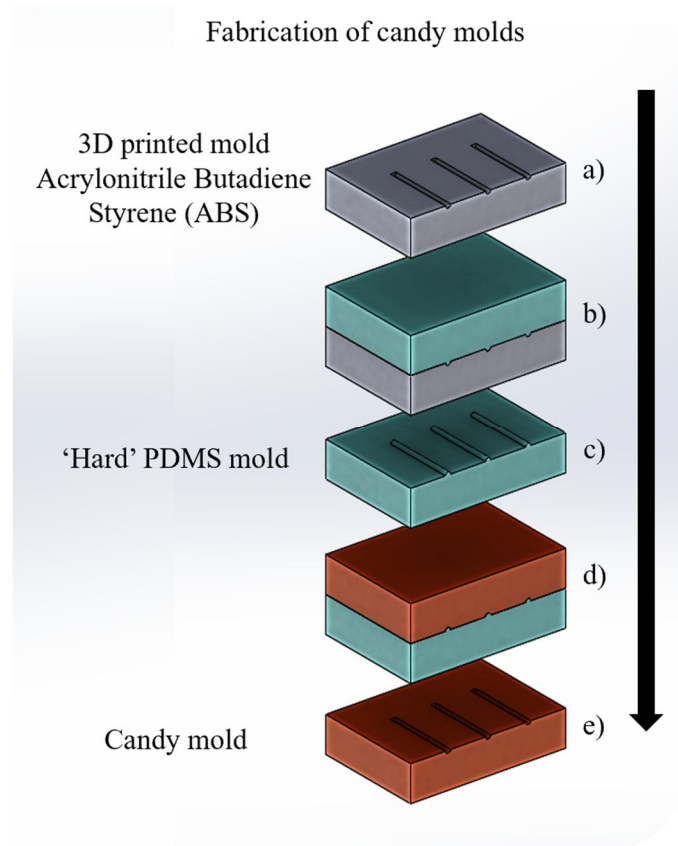


Figure 7 Overview of the steps to fabricate candy molds. a) 3D printed master mold; b) soft lithography to fabricate hard-PDMS mold; c) hard-PDMS mold; d) super soft lithography to fabricate candy mold; e) Candy mold.

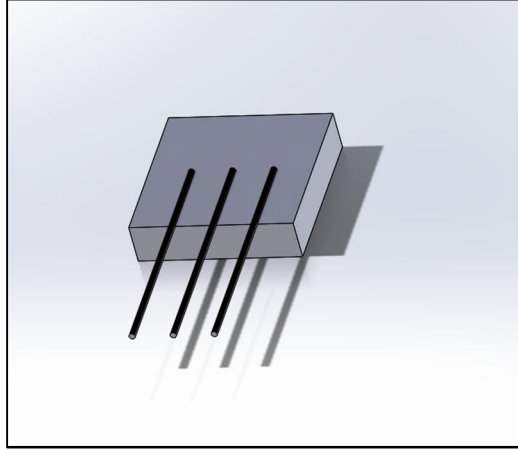


Figure 8 CAD model of carbon microelectrodes array used for the injection molding process.

### Injection Molding Process

Injection Molding follows the three common steps to all injection molding processes. The initial stage is filling the mold with the material desired to create polymer parts. This step was achieved by filling the microchannels with soft-silicone using the apparatus shown in figure 9. Candy mold was placed on a movable platform and aligned with the syringe attached to a micromanipulator. The microchannels were filled by placing the needle into the microchannel. The needle was moved along the length of the microchannel by manually manipulating the movable platform. The microscope was used to visualize the needle in the microchannel. Ejection of the soft-silicone pre-polymer was done controllably by activating and deactivating the fluid dispensing system connected to a nitrogen compress gas. A pressure of  $\sim 32$  kPa was enough to eject the soft-silicone into microchannels.

After filling, the candy mold was transferred to a glass slide and the electrode array was aligned in the mold and taped with polyimide tape to fix the position. The next step is curing. The glass slide was placed in an oven at  $60^{\circ}\text{C}$  to cure soft-silicone

overnight. The final step was demolding. The glass slide was removed from the oven and placed in a hot warm water bath for about 1h at 60°C. Candy molds were dissolved, and carbon microelectrodes were coated with soft-silicone.

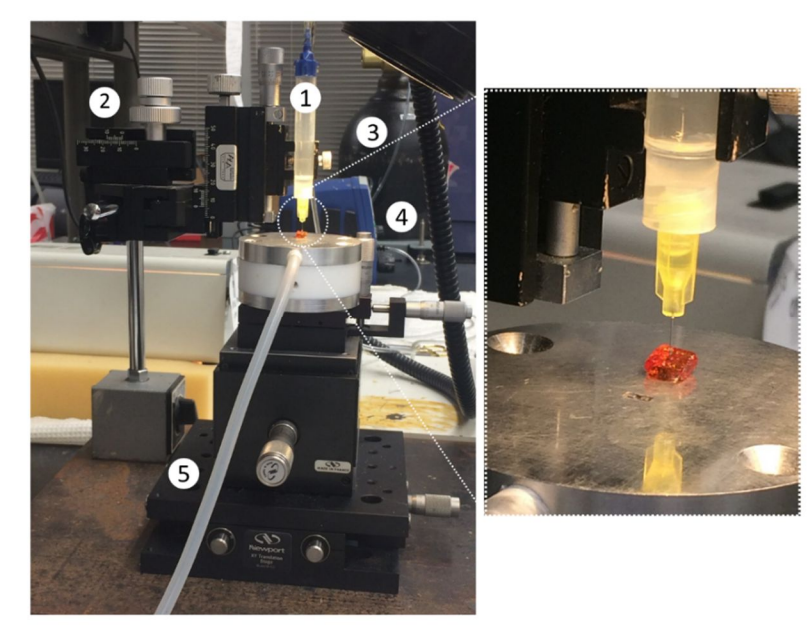


Figure 9 Shows the apparatus utilized for filling the candy molds with soft-silicone. 1) Syringe filled with soft-Silicone; 2) Micromanipulator; 3) Nitrogen compressed gas cylinder; 4) Ultimus I Fluid dispensing system (EFD); 5) Movable platform.

### Setup for Imaging Soft-Silicone Coatings and Analysis

A custom-build image setup was utilized to observe the coating along the diameter of the carbon probes. A centrifuge tube (50ml) was cut around 4mm away from the tip and taped to a platform. A lock lock syringe was used to lock a dispenser needle and then placed inside of the centrifuge tube. The edge of the syringe was taped to increase surface contact to better control the rotation of the syringe in the centrifuge tube. Then, the tip of the dispenser needle was attached to a circular plastic part with an inner diameter of  $\sim 1$ mm. Finally, a polyimide tube is inserted in the inner diameter of the circular plastic to serve as a support for the carbon microelectrodes to be imaged. A LED

light 100X200X USB digital microscope was used to take images. Coating uniformity was evaluated by measuring and averaging the thicknesses of 10 different regions along the length of each electrode (n=12) before and after 90 degrees rotation. Images were analyzed using ImageJ.

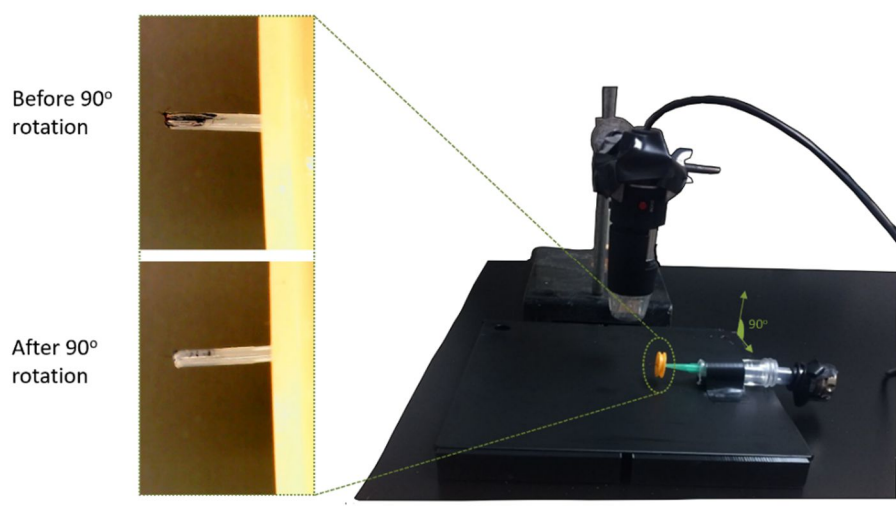


Figure 10 Custom-build image setup to image coated carbon electrodes.

## RESULTS

### Candy Molds

It was observed that candy molds were able to mimic all features of the ABS master mold. As seen in figure 11, not only the microchannels pattern was transferred, but also, the surface rugosity of the master mold.



Figure 11 Shows the fidelity of pattern transferring using super soft lithography. From left to right, ABS master mold, hard-PDMS mold and candy mold.



## Soft-Silicone Coated Carbon Microelectrodes

To test the scalability of the process, 30 carbon microelectrodes were coated in the same batch. At the end of the process, it was noticed that all carbon fibers were successfully coated. Examples of coated carbon fibers can be seen in figure 12. The coating thickness before and after rotation can be seen in figure 13. The total average thickness of all 12 electrodes before rotation was 0.397 millimeters with standard deviation of 0.070 millimeters. After 90 degrees of rotation, the total average thickness was 0.442 millimeters with standard deviation of 0.062 millimeters. The difference between both average thicknesses is lesser than their respective variance and, therefore, it can be said that coating was uniform in all 12 electrodes.

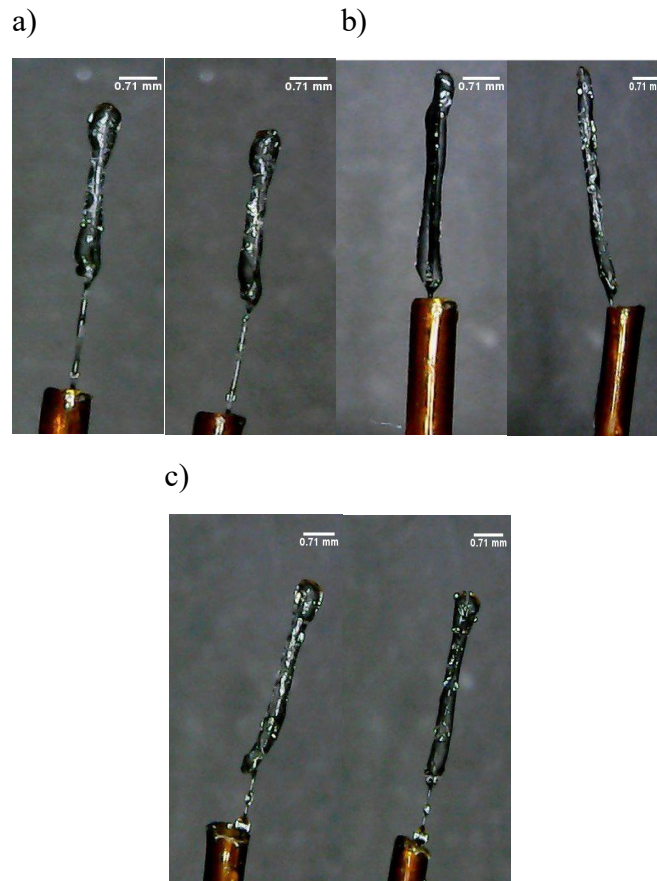


Figure 12. Displays samples of carbon electrodes coated with soft-silicone before (left) and after (right) 90 degrees of rotation. a) electrode 1, b) electrode 2 and c) electrode 3.

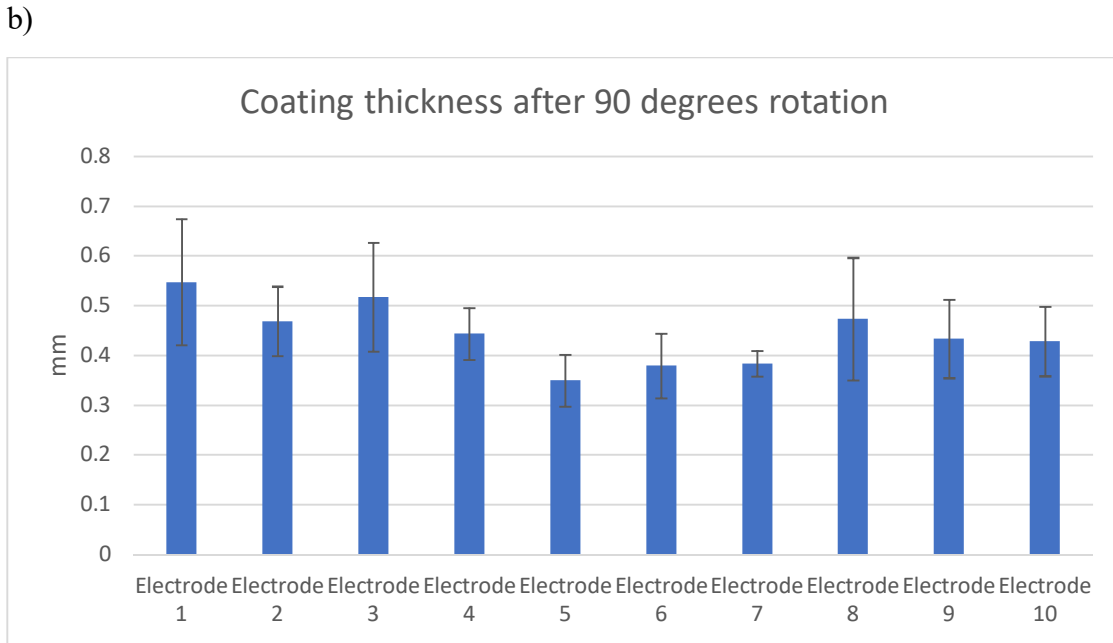
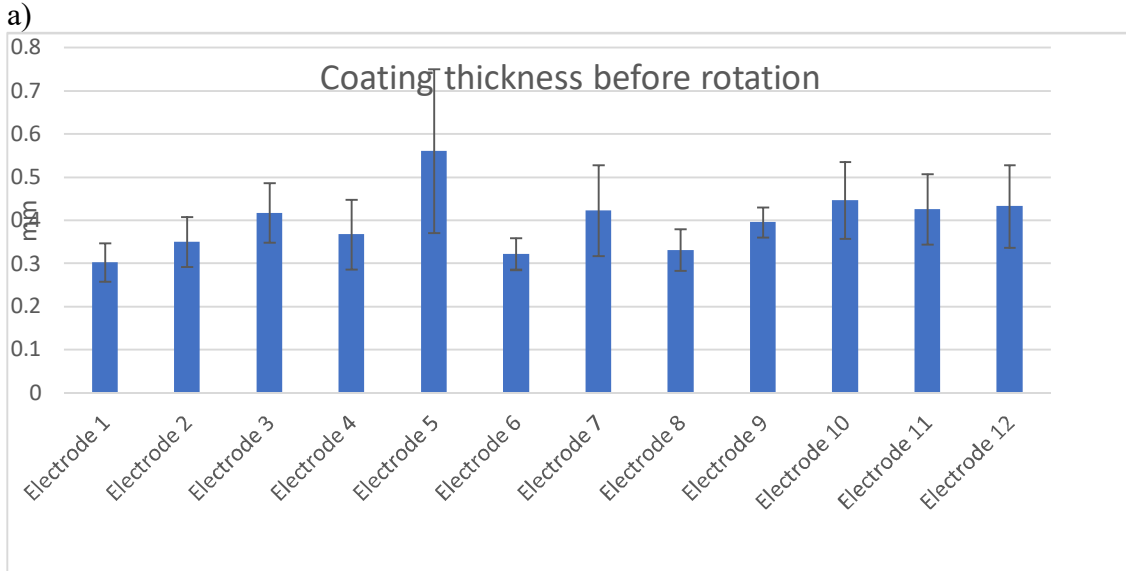


Figure 13. Graphs of coating thickness of 10 electrodes before (a) and after (b) 90 degrees of rotation.

### Discussion

The data indicate that avoiding mechanical stresses during demolding, microelectrodes can be successfully coated with ultra-soft polymer. This was achieved

because candy-molds exhibited faithful replication of microchannels pattern from ABS master mold. But, two precautions needed to be taken to maintain the high-fidelity of candy molds. They needed to be stored in a low humidity environment until further use because moisture make them lose its rigidity, thus losing their pattern. Also, curing temperature cannot be greater than 70°C because candy loses its rigidity at high temperatures. All these observations agree with previously observations in [25]. Moreover, it was noticed that coating presented a small variability in its uniformity. Two potential causes of variability were identified, the ABS master mold and filling step. It was verified that Stratasys Mojo machine is not capable of precisely creating microchannels with a diameter of ~350 microns (data not shown). As a result, diameter is not consistent throughout microchannels length. In respect to filling step, soft-Silicone may overflow microchannels causing an increase of coating dimensions if the needle is not carefully aligned in the channel or if the injection of soft-Silicone is not done controllably.

#### Conclusion and future work

The soft coating injection molding process proved to be feasible to coat multiple microelectrodes per batch (n=30). This was achieved by manufacturing a water-soluble candy mold to avoid mechanical stresses around soft coating during its demolding. It is important to mention that this method can also fabricate thinner coatings if the dimensions of microchannels are reduced. Although the candy mold proved to be a low-cost visible alternative for the soft microinjection molding process, it is the current

limiting factor for fast production since it not resistant to high-temperatures. Therefore, future work will pursue solutions for fast manufacturing.

## CHAPTER 3

### STABILITY STUDIES OF SOFT-SILICONE LOADED WITH PDMSO

#### Outline

It is of importance to investigate the chronic stability of soft-silicone coating loaded with PDMSO to assure that neural interface is capable of sensing  $pO_2$  long-term. Here, instability is addressed as any situation that would prevent stable  $pO_2$  sensing around and along carbon microelectrode using the MR-PISTOL technique. Many factors may contribute to coating instability in neural tissue. Two potential factors were investigated, the delamination of the coating during implantation of carbon electrode into neural tissue and the loss of siloxanes of PDMSO from the coating over time. If coating delamination occurs, a conformal coating around carbon electrode could not be guaranteed. Hence,  $pO_2$  measurements around and along carbon electrode length would not be physically achievable. In relation to the loss of PDMSO, without their presence in the soft-silicone coating, MR-PISTOL imaging could not be performed. Though previous study attested that the soft-silicone loaded with PDMSO provided stable  $pO_2$  spatial-temporal maps for at least a month in *in vivo* mouse brain (see Chapter 2), it is necessary to search for alternative techniques to MR-PISTOL to quantitatively evaluate potential PDMSO diffusion into neural tissue.

## MATERIALS AND METHODS

All animal procedures were done under Arizona State University Institutional Animal Care & Use Committee (IACUC) 1492 and 1535 for rat and mouse, respectively.

Contact for public release of the protocols is in following website:

[researchintegrity.asu.edu/animals](http://researchintegrity.asu.edu/animals)

### Preparation of Soft-Silicone Coated Carbon microelectrodes for Animal Experiments

Soft-silicone coated carbon electrodes were fabricated as described in chapter two. After fabrication, they were stored in deionized water (DI) until implantation. A total of two coated carbon electrodes were utilized for each animal experiment (n= 3 animals). One control (soft-silicone unloaded with PDMSO) and one sample (soft-silicone loaded with PDMSO). Prior to surgery, coated carbon electrodes (length ~ 4mm) were removed from DI and mounted individually on a glass slide with polyimide tape. Both control and sample probes were kept in artificial cerebrospinal fluid (acsf) prior to implantation. But, prior to immersion in acsf, sample probes were first loaded with PDMSO by dipping the coated carbon electrodes into a Eppendorf tube (1.5ml) containing PDMSO.

### Preparation of artificial cerebrospinal fluid

The artificial cerebrospinal fluid (acsf) was made according to the following recipe. 7.4 grams of sodium chloride, 2.1 grams of sodium bicarbonate, 0.17 grams of sodium phosphate monobasic, 0.19 grams of magnesium chloride and 4.5 grams of glucose were mixed and diluted in one liter of (DI).

## SURGERIES PROCEDURES FOR ACUTE ANIMAL EXPERIMENTS

Transmission Electron Microscopy (TEM) and Scanning Electron Microscope (SEM) with Energy Dispersive X-ray (EDS) Analysis

Adult male mouse, species *Mus musculus* (strain C57BL/6) weighing 50 grams was first anesthetized using a ketamine/xylazine/acepromazine (kxa) cocktail for induction. The head region superior to the skull was fully shaved and triple swabbed using 70% ethanol. Then, the mouse head was mounted in the ear bars of the stereotaxic frame. Ointment was applied on the eyes to keep them from drying during surgery. After incision, the skin flaps were pulled away and the skull surface cleaned using a combination of cotton swabs and 2% hydrogen peroxide (v/v). A craniotomy (~5mm diameter) was done by carefully drilling a hole on the skull on either hemisphere (2.5mm post bregma). Then, the removal of the skull and dura were done to expose the brain cortical surface. The coated carbon fibers were mounted on a stereotactic manipulator and inserted into the cortex. The control coated carbon fiber and the sample coated carbon fiber were inserted in opposite hemispheres. Using the sagittal suture as a reference, the control was placed in the left hemisphere and the sample in the right hemisphere. Their penetration depth was approximately 3mm. Probes stayed in the brain for about 6 hours. Saline solution was administered on top of the brain via syringe to maintain the hydration of the brain. After 6 hours, mouse was euthanized, and the head was decapitated. The brain was extracted and was placed in cold acsf (4°C). The neural tissue containing the probes was excised (~0.5cm (w×l×h) cube). These tissue samples were prepared following TEM protocol described in appendix A. Specimens were analyzed using JEOL 2010F TEM and SNE-4500 M tabletop SEM.

### 3D X-ray imaging

Sprawling dawlley male rat weighting approximately 250 grams was anesthetized, and craniotomy was performed similarly to the one reported in TEM/SEM acute experiment. Carbon fibers coated with loaded and unloaded soft-silicone were implanted ~2.5 mm post bregma in the right hemisphere after removal of dura. Subsequently, the animal was euthanized, and the entire brain was excised and placed in a petri dish containing cold acsf (4°C) and transported to the imaging location. At the imaging location site, the brain was transferred to a small plastic container filled with acsf. The container was closed with paraffin film and positioned in the 3D X-ray microscope (ZEISS Xradia 520 Versa).

### Surgery Procedure for Scanning Electron Microscope (SEM) with Energy Dispersive X-ray Analysis (SEM/EDS) Chronic Animal Experiment

Adult male mouse, species *Mus musculus* (strain C57BL/6) was used. The surgical preparation was similar to the one described in TEM/SEM acute experiment section. Multiple (4) craniotomies (~2mm diameter) were done by carefully drilling a hole on the skull on either hemisphere centered 2.5mm post bregma and 2.5 mm anterior to the bregma. After insertion of the probes, the holes in the skull were filled with GelFoam and covered with a polyester film which was then secured with bone cement. Implantable probes stayed in the mouse brain for about 2 weeks. After 2 weeks, the animal was euthanized, and the brain was harvested as previously described for the TEM/SEM procedure. The sample preparation of extracted brain slices was done according to critical point drying protocol detailed in Appendix A. Specimen were evaluated using SNE-4500 M tabletop SEM.

## ENERGY DISPERSIVE X-RAY ANALYZES

### Background

Energy dispersive X-ray Analysis (EDS) is an analytical technique used for the identification of chemical elements constituent of a sample. In brief, EDS technique relies on the detection of x-rays emitted from a sample due to the bombardment of a high energy electron beam. These x-rays are characteristic to each chemical element and are resulted from electron transitions between electron shells of the element. This ionization happens because of the bombardment of electrons. EDS graphs are usually represented by a spectrum of x-ray energy (keV) on an x-axis and relative abundance of emitted x-rays on the y-axis. To recognize the existence of a certain chemical element in the sample, x-ray characteristics peaks of the element should be seen on EDS graph. For example, if we would like to detect silicon, peaks at 1.740 keV (represents the energy of  $K_{\alpha 1}$ ) or 1.873 keV (represents the energy of  $K_{\beta 1}$ ) should be observed and distinguished statistically from background fluctuations. This background is a continuum x-ray often called bremsstrahlung. It denotes the deceleration of the electrons from the electron beam when they interact with the electric field that surrounds the nuclei of atoms in the sample.

### Criterion for Brain Tissues Silicon Analyzes

Raw EDS data were analyzed from both JEOL 2010F TEM and SNE-4500 M table top SEM machines. Identification of silicon presence in brain slices was done by observing at least one of the silicon characteristic peaks. The assumption is silicon would indirectly indicate PDMSO leakage.



## RESULTS

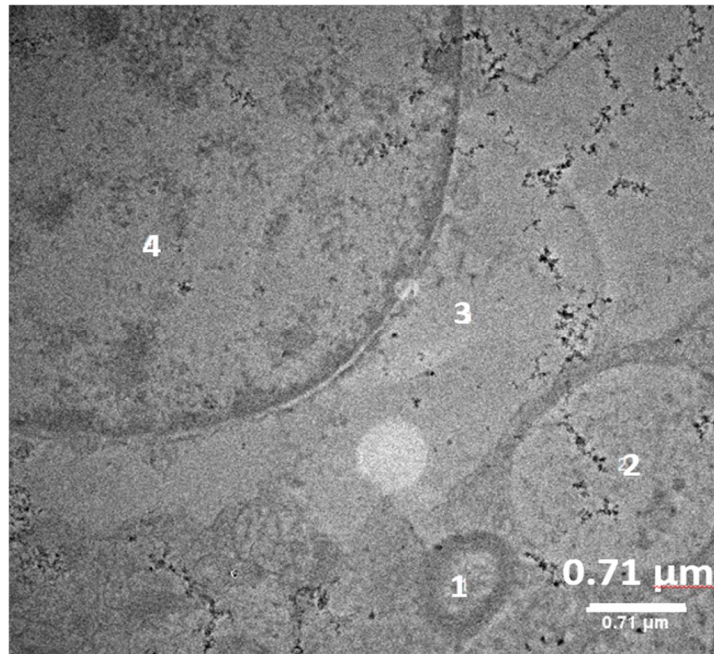
### ANALYSIS OF BRAIN SLICES

#### TEM/EDS Analysis of Acute Animal Experiment

Brain slices containing puncture of control coated carbon electrode (control brain tissue) and puncture of sample coated carbon electrode (sample brain tissue) were analyzed. Different sampling points were chosen for the EDS analysis. A random portion of the control brain tissue was analyzed because puncture was not successfully found. The sampling points of brain sample tissue were close to the puncture. Control brain tissue partial data can be seen in figure 14 as an example of acquired TEM image and EDS spectrum. For more TEM images and EDS spectrums, please refer to Appendix A.

Counts of silicon and osmium from all EDS spectrums were grouped in Table 1 to assist data visualization and interpretation. Osmium was also evaluated because one of its peaks (1.907 keV) is nearby to the silicon peak at 1.873 keV. Overall, in the presence of osmium, the silicon peak at 1.873 keV is very difficult to identify because osmium peak is dominant. In respect to the silicon peak at 1.740 keV, both the control and sample brain tissues presented with a silicon peak. Although peaks were small (less than 400 counts as noticed with osmium), they were higher (point 1 overpassed 200 counts and points 2 to 4 were close to 200 counts) and well-defined in the sample brain tissue.

a)



b)

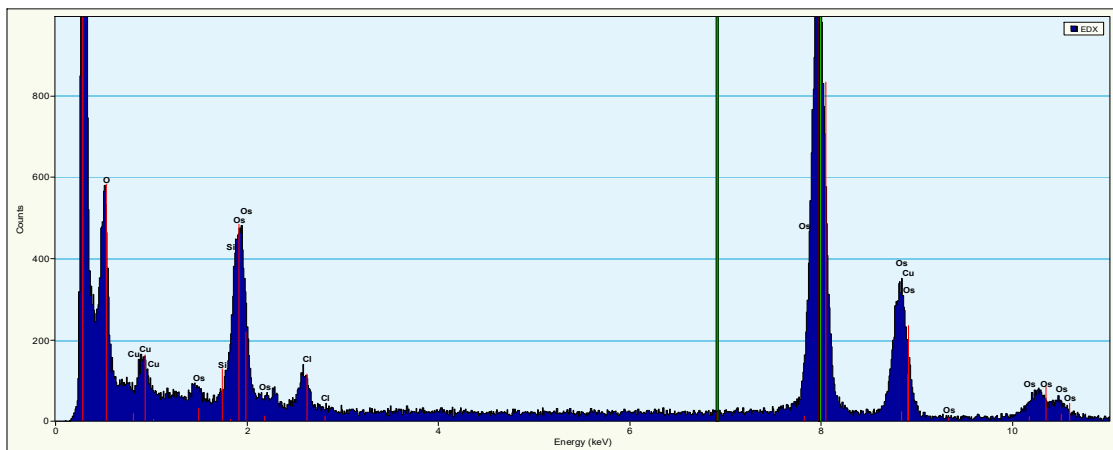


Figure 14 a) TEM imaging of a random region of the control brain tissue. b) EDS spectrum from sampling point 1. A well-defined peak of silicon was not detected. But osmium peak was, and it was greater than 400 counts.

Table 1. Summary of silicon and osmium counts from all EDS sampling points.

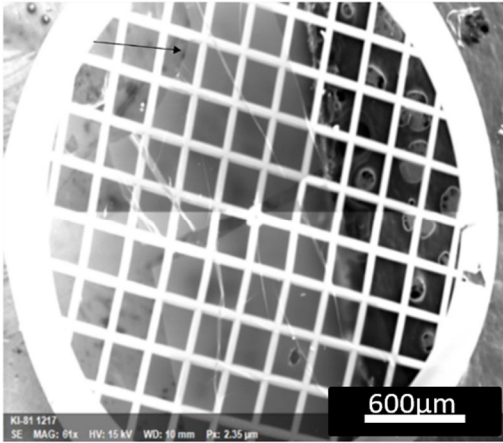
	Si K $\alpha$ 1 (1.740 keV) Peak				Os M $\alpha$ 1 (1.907 keV) Peak			
	Point 1	Point 2	Point 3	Point 4	Point 1	Point 2	Point 3	Point 4
Soft PDMS (Control)	-	<< 200 counts	<< 200 counts	<< 200 counts	> 400 counts	<400 counts; close to 400 counts	<400 counts; close to 200 counts	<< 200 counts
Soft-PDMS/PDMSO (Sample)	> 200 counts; close to 200 counts	< 200 counts; close to 200 counts	< 200 counts; close to 200 counts	not counted	< 400 counts; close to 400 counts	-	-	not counted

### SEM/EDS Analysis of Acute Animal Experiment

For SEM/EDS analysis, only the sample brain tissue was imaged. The SEM images were done with two different accelerated voltages, 15.0 keV and 5 keV. The SEM image done at 15.0 keV imaged the whole sample brain tissue, whereas, at 5 keV only imaged the surrounding area of the puncture. The EDS mapping of silicon at 15.0 keV can be seen in figure 15 and its respective EDS spectrum is shown in figure 16. The EDS analysis of SEM image at 5 keV can be observed in figure 17.

EDS spectrum of the whole sample brain tissue (figure 16 (b)) displayed a silicon peak around 1.740 keV. But, EDS software from SEM did not recognize as a detectable element (see table in figure 16 (b)). Moreover, it was noticed that EDS mapping of silicone (figure 16 (a)) mostly matches the copper grid structure. This may indicate that silicon mapping was not accurate and cannot be trusted with confidence. Furthermore, the EDS analysis of brain tissue surrounding puncture (figure 18) exhibited similar results even though the x-ray background significantly decreased.

a)



b)

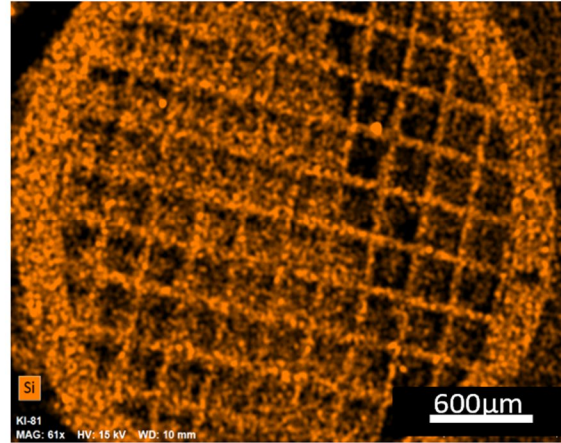
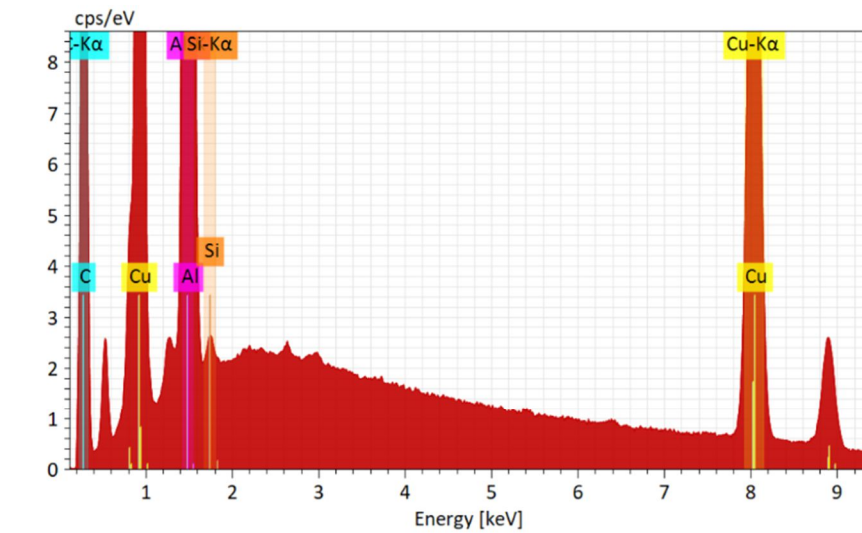


Figure 15 Shows in (a) the SEM image of the sample brain tissue done at 15.0 keV and 61x magnified. The electrode puncture is located at the top left (see black arrow) b) the EDS mapping of silicon.

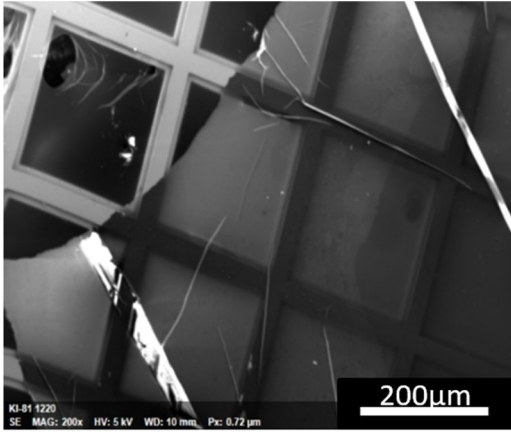


Map

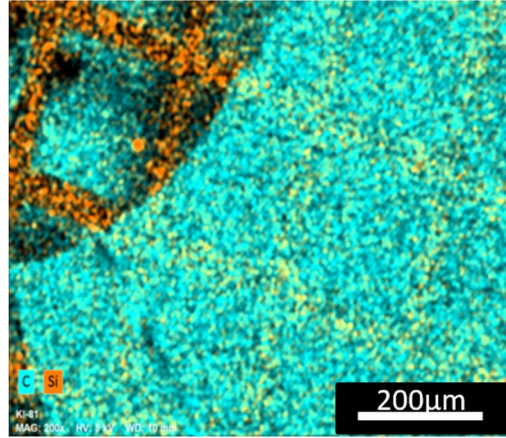
Element	At. No.	Netto	Mass [%]	Mass Norm. [%]	Atom [%]	abs. error [%] (1 sigma)	rel. error [%] (1 sigma)
Carbon	6	216703	23.75	24.38	54.45	2.60	10.96
Aluminium	13	1351497	23.19	23.81	23.67	1.10	4.73
Silicon	14	0	0.00	0.00	0.00	0.00	2.15
Copper	29	466975	50.48	51.82	21.88	1.61	3.19
		<b>Sum</b>	<b>97.42</b>	<b>100.00</b>	<b>100.00</b>		

Figure 16 Displays the EDS spectrum of the whole sample brain tissue and the EDS analyses done by the SEM software.

a)



b)



c)

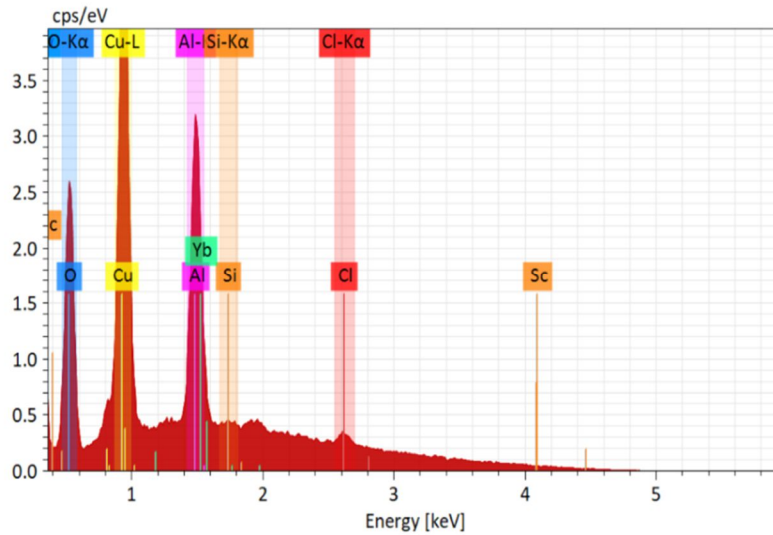


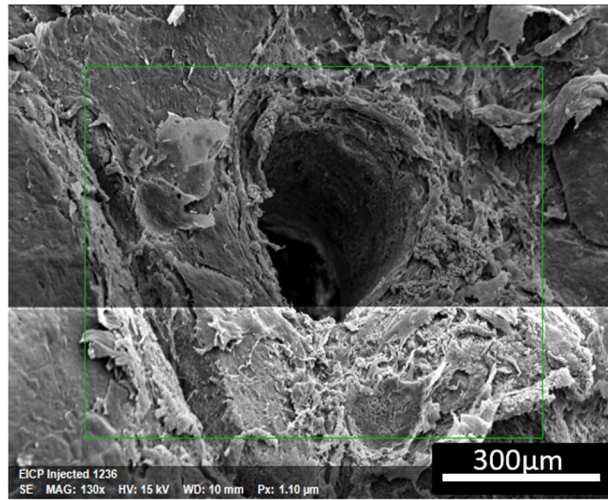
Figure 17 a) SEM imaging at 5 keV of the sample brain tissue puncture 200x magnified. b) EDS mapping of silicon and carbon. c) EDS spectrum of the brain tissue surrounding the puncture.

### Analysis of Chronic Animal Experiment

The SEM imaging and EDS spectrum of control and sample brain tissue can be seen in figure 18 and figure 19, respectively. The EDS data of both displayed a peak close to a typical silicon peak at 1.873 keV. This peak was more pronounced in the EDS

spectrum of control brain tissue. Since this peak is not located exactly at 1.873 keV, we cannot say with certainty that silicon is present in both brain tissues.

a)



b)

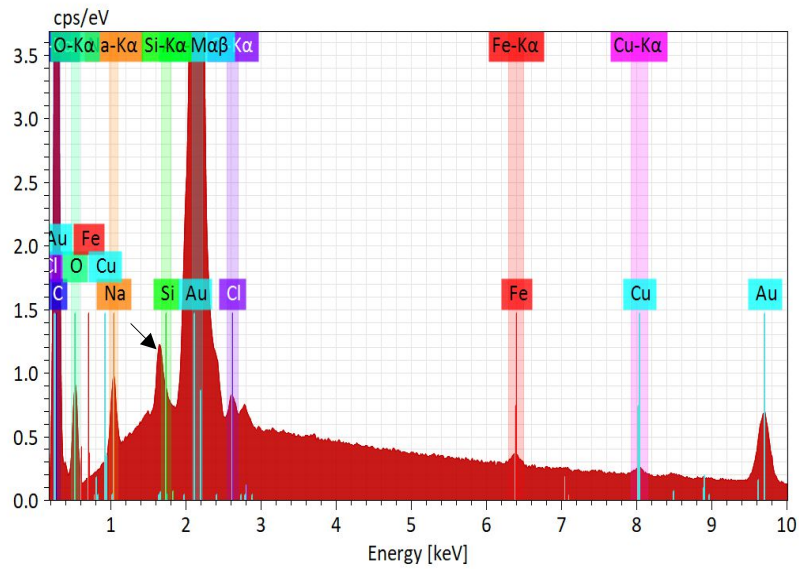
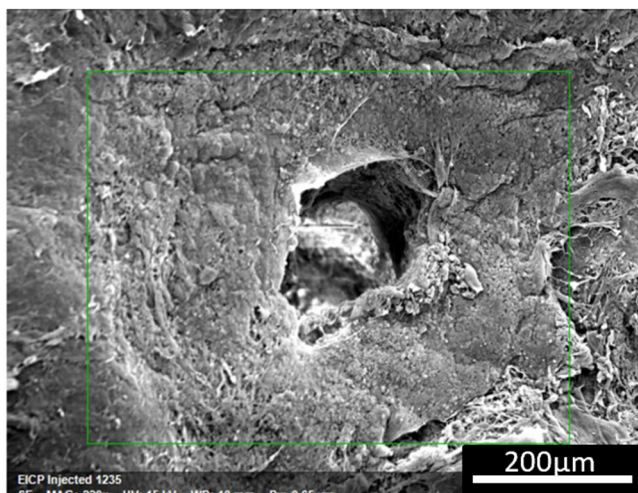


Figure 18 a) SEM imaging with magnification of 130x at 15 kV showing the electrode track of control brain tissue. b) the EDS spectrum of the control brain tissue.

a)



b)

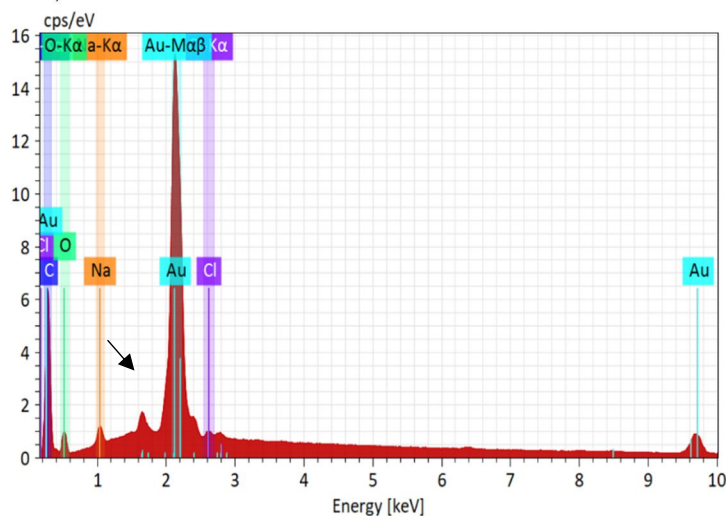


Figure 19 a) SEM imaging with magnification of 220x at 15 kV exposing the electrode track sample brain tissue. b) the EDS spectrum of the sample brain tissue.

## Study of Mechanical Integrity of Control and Sample Coated Carbon Microelectrodes in Ex-Vivo Rat Brain

Control coated carbon electrode showed successful insertion, see left arrow in figure 18. Its coating-maintained uniformity and integrity. Contrarily, the coating of

sample carbon microelectrode delaminated during insertion, see right arrow in figure 20.

It was also observed that delaminated coating stayed on top of the brain.

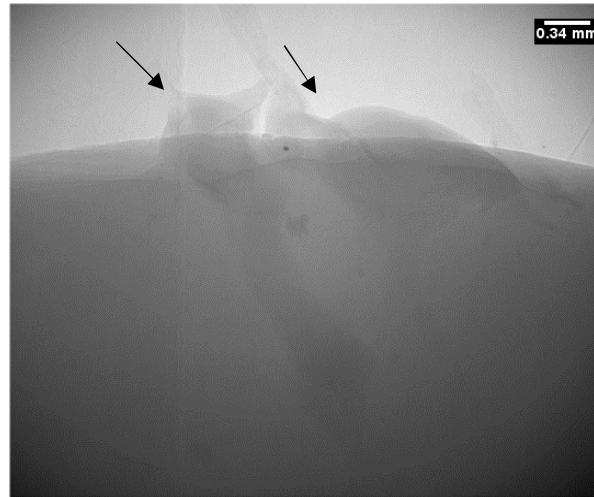


Figure 20 3D x-ray of coated carbon microelectrodes implanted in the cerebral cortex of the rat brain. Coated carbon fiber unloaded with PDMSO is seen under the black arrow on left and the coated carbon fiber loaded with PDMSO is seen under the black arrow on the right.

## Discussion

TEM/EDS analysis of control and sample brain tissues from acute chemical stability experiment detected a low concentration of silicon. But the sample brain tissue had higher silicon counts.

One of the possible reasons for this is the location of sampling points. Since the points in the sample tissue were closer to the carbon electrode puncture, these silicones probably came from the soft-silicone coating that was left behind during probe extraction. Thus, in this case, a positive detection of silicon does not necessarily translate to PDMSO presence in the brain tissue.

Regarding the silicon peak found in control tissue, it was unclear where it came from because EDS measurements were not done close to the electrode track. This



observation may suggest that brain tissue has a silicon peak ‘background’. Kappel et al. [26] studied tissue samples from a patient who had a gel bleed from her silicone breast implants for 17 years. TEM/EDS was one of the analyses done to spot silicone presence in different tissue samples. They observed that all control tissues of patients without silicone breast implants had a silicon peak ‘background’ below 500 net counts.

Translating the Kappel’s group finding to this work, the silicon peak that was observed in the TEM/EDS analysis of the control brain tissue may be a silicon ‘background’ of the mouse brain which might not be related to a potential diffusion of PDMSO.

The SEM/EDS analysis of control and sample brain tissues from both, acute and chronic experiments, did not traced silicon distribution on the surface of analyzed slices. These results pinpoint that PDMSO absorbed in the soft-silicone coating did not diffused to the brain tissue. Yet SEM/EDS analysis might not be conclusive. The fact that support this affirmation is the ambiguous results saw in the TEM/EDS and SEM/EDS analysis of the same sample brain tissue. As mentioned in the results section, TEM/EDS analysis was able to find silicon while SEM/EDS analysis was unable of measuring it. The tissue thickness (~ 200 nm) may had compromised the capability of SEM/EDS in measuring this small concentration of silicon.

In relation to the coating mechanical stability study, data indicated a likely mechanical instability of the soft-silicone loaded with PDMSO. Sample coated carbon microelectrodes used in chemical stability studies did not delaminated. Thus, this mechanical stability of the coating was not expected, and it was unclear why it occurred. Many factors may contribute to mechanical stability of the coating, such as factors

intrinsically related to the coating fabrication process or quantity of loaded PDMSO in the coating.

#### Conclusion and Future Work

Carbon microelectrodes coated with soft-silicone loaded and unloaded with PDMSO were tested under acute and chronic conditions for studying their biostability in the brain. Two approaches, TEM/EDS and SEM/EDS analysis were exploited to investigate if PDMSO leaches out of the soft-silicone coating after exposure to brain environment. Both methods were proved to be feasible for imaging brain tissue and performing EDS. But there are advantages and drawbacks with each method. TEM imaging provide good resolution but poor contrast imaging, making it difficult to recognize the spatial location of the electrode track. However, it can detect relatively small amounts of silicone. SEM/EDS has the advantage of carrying out EDS mapping throughout the surface, which could be useful to observe PDMSO diffusion profile in the nervous tissue. Nevertheless, its detection limit should be further investigated to assure that non-detection of silicon is not due to the detection limit of SNE-4500 M.

Moreover, the initial EDS analysis of both, TEM and SEM, relied on the assumption that silicon presence in the brain tissue is directly related to a possible diffusion of PDMSO. Since other silicon sources may exist and sample preparation may confound the results due to tissue processing, it would be of interest to test alternative methods such as gas chromatography/mass spectroscopy [27] or Fourier-transform infrared spectroscopy (FT-IR) [28] to certify that PDMSO is (i) the exclusive source of silicon in the brain or (ii) the sample preparation does not affect PDMSO presence, in case of leaching out into brain environment.

The result of the mechanical stability studied indicated that coating loaded with PDMSO is mechanically unstable. However, electrodes used in the chemical stability studies were successfully implanted in the mouse brain. Further experiments should be done to better understand causes of failure to circumvent possible mechanical instability of soft-silicone loaded with PDMSO.

## REFERENCES

- [1] J. P. Lowry, K. Griffin, S. B. McHugh, A. S. Lowe, M. Tricklebank, and N. R. Sibson, "Real-time electrochemical monitoring of brain tissue oxygen: A surrogate for functional magnetic resonance imaging in rodents," *Neuroimage*, vol. 52, no. 2, pp. 549–555, 2010.
- [2] A. Ledo, C. F. Lourenço, J. Laranjinha, C. M. A. Brett, G. A. Gerhardt, and R. M. Barbosa, "Ceramic-Based Multisite Platinum Microelectrode Arrays: Morphological Characteristics and Electrochemical Performance for Extracellular Oxygen Measurements in Brain Tissue," *Anal. Chem.*, vol. 89, no. 3, pp. 1674–1683, 2017.
- [3] E. Ortiz-Prado, S. Natah, S. Srinivasan, and J. F. Dunn, "A method for measuring brain partial pressure of oxygen in unanesthetized unrestrained subjects: The effect of acute and chronic hypoxia on brain tissue PO<sub>2</sub>," *J. Neurosci. Methods*, vol. 193, no. 2, pp. 217–225, 2010.
- [4] J. I. Peterson, R. V. Fitzgerald, and D. K. Buckhold, "Fiber-Optic Probe for in Vivo Measurement of Oxygen Partial Pressure," *Anal. Chem.*, vol. 56, no. 1, pp. 62–67, 1984.
- [5] C. Zhang, S. Bélanger, P. Pouliot, and F. Lesage, "Measurement of local partial pressure of oxygen in the brain tissue under normoxia and epilepsy with phosphorescence lifetime microscopy," *PLoS One*, vol. 10, no. 8, pp. 1–14, 2015.
- [6] A. Carreau, B. El Hafny-Rahbi, A. Matejuk, C. Grillon, and C. Kieda, "Why is the partial oxygen pressure of human tissues a crucial parameter? Small molecules and hypoxia," *J. Cell. Mol. Med.*, vol. 15, no. 6, pp. 1239–1253, 2011.
- [7] A. Gersten, J. Perle, A. Raz, and R. Fried, "Probing brain oxygenation with near infrared spectroscopy," *NeuroQuantology*, vol. 7, no. 2, pp. 258–266, 2009.
- [8] J. Weaver and K. Liu, "In vivo electron paramagnetic resonance oximetry and applications in the brain," *Med. Gas Res.*, vol. 7, no. 1, p. 56, 2017.
- [9] V. D. Kodibagkar, X. Wang, J. Pacheco-Torres, P. Gulaka, and R. P. Mason, "Proton imaging of siloxanes to map tissue oxygenation levels (PISTOL): a tool for quantitative tissue oximetry," *NMR Biomed*, vol. 21, no. 8, pp. 899–907, 2008.
- [10] R. Green and M. Reza Abidian, "Conducting Polymers for Neural Prosthetic and Neural Interface Applications," *J. Adv. Mater.*, 2015.
- [11] M. J. Sridharan A, "Performance of soft, brain-like neural implants in rodents in chronic experiments.," *Front Bioeng Biotechnol*.
- [12] J. Beauchamp, "Quantitatively Assessing Levels of Oxygen at Neural Interface with MR Techniques; A Feasibility Study," Arizona State University.
- [13] V. Guarino, S. Zuppolini, A. Borriello, and L. Ambrosio, "Electro-active polymers (EAPs): A promising route to design bio-organic/bioinspired platforms with on

- demand functionalities,” *Polymers (Basel)*., vol. 8, no. 5, 2016.
- [14] Liang Guo, G. S. Guvanasen, Xi Liu, C. Tuthill, T. R. Nichols, and S. P. DeWeerth, “A PDMS-based integrated stretchable microelectrode array (isMEA) for neural and muscular surface interfacing.,” *IEEE Trans. Biomed. Circuits Syst.*, vol. 7, no. 1, pp. 1–10, 2013.
- [15] Y. X. Kato, S. Furukawa, K. Samejima, N. Hironaka, and M. Kashino, “Photosensitive-polyimide based method for fabricating various neural electrode architectures,” *Front. Neuroeng.*, vol. 5, no. May 2014, 2012.
- [16] D. H. Kim, J. A. Wiler, D. J. Anderson, D. R. Kipke, and D. C. Martin, “Conducting polymers on hydrogel-coated neural electrode provide sensitive neural recordings in auditory cortex,” *Acta Biomater.*, vol. 6, no. 1, pp. 57–62, 2010.
- [17] A. Weltman, J. Yoo, and E. Meng, “Flexible, penetrating brain probes enabled by advances in polymer microfabrication,” *Micromachines*, vol. 7, no. 10, 2016.
- [18] H. N. Schwerdt *et al.*, “Cellular-scale probes enable stable chronic subsecond monitoring of dopamine neurochemicals in a rodent model,” *Commun. Biol.*, vol. 1, no. 1, p. 144, 2018.
- [19] M. R. Abidian and D. C. Martin, “Multifunctional nanobiomaterials for neural interfaces,” *Adv. Funct. Mater.*, vol. 19, no. 4, pp. 573–585, 2009.
- [20] E. Trikantzopoulos, C. Yang, M. Ganesana, W. Ying, and B. J. Venton, “Novel Carbon-Fiber Microelectrode Batch Fabrication using a 3D-Printed Mold and Polyimide Resin,” *J. Anal.*, 2016.
- [21] M. Lo *et al.*, “Coating flexible probes with an ultra fast degrading polymer to aid in tissue insertion,” *J. Biomed. Microdevices*, 2015.
- [22] V. Goodship, “4 - Injection Molding of Thermoplastics,” in *Design and Manufacture of Plastic Components for Multifunctionality*, V. Goodship, B. Middleton, and R. Cherrington, Eds. Oxford: William Andrew Publishing, 2016, pp. 103–170.
- [23] P. H. Kauffer, *Injection Molding : Process, Design, and Applications*. Hauppauge, UNITED STATES: Nova Science Publishers, Incorporated, 2011.
- [24] “Liquid Injection Molding: Processing Guide for SILASTICTM Liquid Silicone Rubber (LSR) and SILASTICTM FLuoro Liquid Silicone Rubber (F-LSR),” 2012. [Online]. Available: <https://consumer.dow.com/en-us/document-viewer.html?randomVar=8769451049762803006&docPath=/content/dam/dcc/documents/en-us/app-tech-guide/45/45-10/45-1014-01-liquid-injection-molding-processing-guide.pdf>.
- [25] C. Moraes, J. M. Labuz, Y. Shao, J. Fu, and S. Takayam, “Supersoft lithography: Candy-based fabrication of soft silicone microstructures,” *J. Lab Chip*, 2015.
- [26] R. Kappel, L. Boer, and D. H., “Gel Bleed and Rupture of Silicone Breast Implants

Investigated by Light-, Electron Microscopy and Energy Dispersive X-ray Analysis of Internal Organs and Nervous Tissue,” *Clin. Med. Rev. Case Reports*, vol. 3, no. 1, pp. 1–9, 2016.

- [27] S. V. Kala, E. D. Lykissa, and R. M. Lebovitz, “Detection and Characterization of Poly(dimethylsiloxane)s in Biological Tissues by GC/AED and GC/MS,” *Anal. Chem.*, vol. 69, no. 7, pp. 1267–1272, 1997.
- [28] A. Lanzarotta and C. M. Kelley, “Forensic Analysis of Human Autopsy Tissue for the Presence of Polydimethylsiloxane (Silicone) and Volatile Cyclic Siloxanes using Macro FT-IR, FT-IR Spectroscopic Imaging and Headspace GC-MS,” *J. Forensic Sci.*, vol. 61, no. 3, pp. 867–874, 2016.

APPENDIX A

SUPPLEMENTAL MATERIAL FOR CHAPTER III

## PROTOCOLS

### Sample Preparation for Transmission Electron Microscopy (TEM)

Brain slices containing the probes were immersed into vials containing fixation solution of 2% paraformaldehyde/2% glutaraldehyde in 0.1M sodium cacodylate buffer, pH 7.2 for about 15 minutes at room temperature. They were placed on ice for 2 hours. Then, were washed three times for 15 minutes in the same buffer on ice. Samples were post-fixed 1% osmium tetroxide in 0.1M sodium cacodylate buffer, incubated on ice for 2 hours, washed in the same buffer and four times in deionized water, 10 minutes each, at room temperature. Coated carbon fibers were then extracted, and samples incubated in 0.5% aqueous uranyl acetate at 4°C overnight. Next, they were brought to room temperature and washed in deionized water three times, 15 minutes each and dehydrated gradually in a series of ethanol washes (20,40,60,80,100%) where the last step, 100% ethanol, was done 3 times. All steps were done in 10 minutes at room temperature. After dehydration, brain slices were embedded in EPON, epoxy resin and sectioned. Ultra-thin sections (200 nm) were obtained with an ultramicrotome by using an ultra-diamond knife. Brain tissue sections were collected on 3.05 mm 100 mesh copper TEM grids and coated with carbon (thickness  $\sim 50\text{\AA}$ ).

### Sample Preparation for Scanning Electron Microscope SEM via Critical Point Drying

Brain slices are first immersed into vials containing 4% paraformaldehyde in 0.1 M phosphate buffer overnight at 4°C. After fixation in paraformaldehyde, they were brought to room temperature and transferred to vials containing fixation solution of 2.5% glutaraldehyde in 0.1M sodium phosphate and 0.15 M sodium chloride, pH 7.2 for about 2 hours. Then, they were washed in same buffer three times, 10 minutes each. After, brain slices were placed on a Petri dish and manually cut for reducing their height. Also, coated carbon fibers were removed. After cutting, they were transferred to vials for dehydration in a series of ethanol washes (10,20,50,75,100%). All steps were done 10 minutes each, except 10% and 20% which had 5 minutes of duration. The last step, 100% ethanol, was



done 3 times. In sequence, brain slices were put in perforated Eppendorf (1.5ml) tubes which were then placed in Balzers CPD020 machine for critical point drying. The intermediate fluid utilized was ethanol. The replacement of ethanol with liquid carbon dioxide was done 6-7 cycles prior to rinsing temperature to the critical point of carbon dioxide. Next, brain slices were coated with gold (thickness ~150nm) using Technics Sputter Coater.

TEM/EDS ANALYSIS OF ACUTE ANIMAL EXPERIMENT

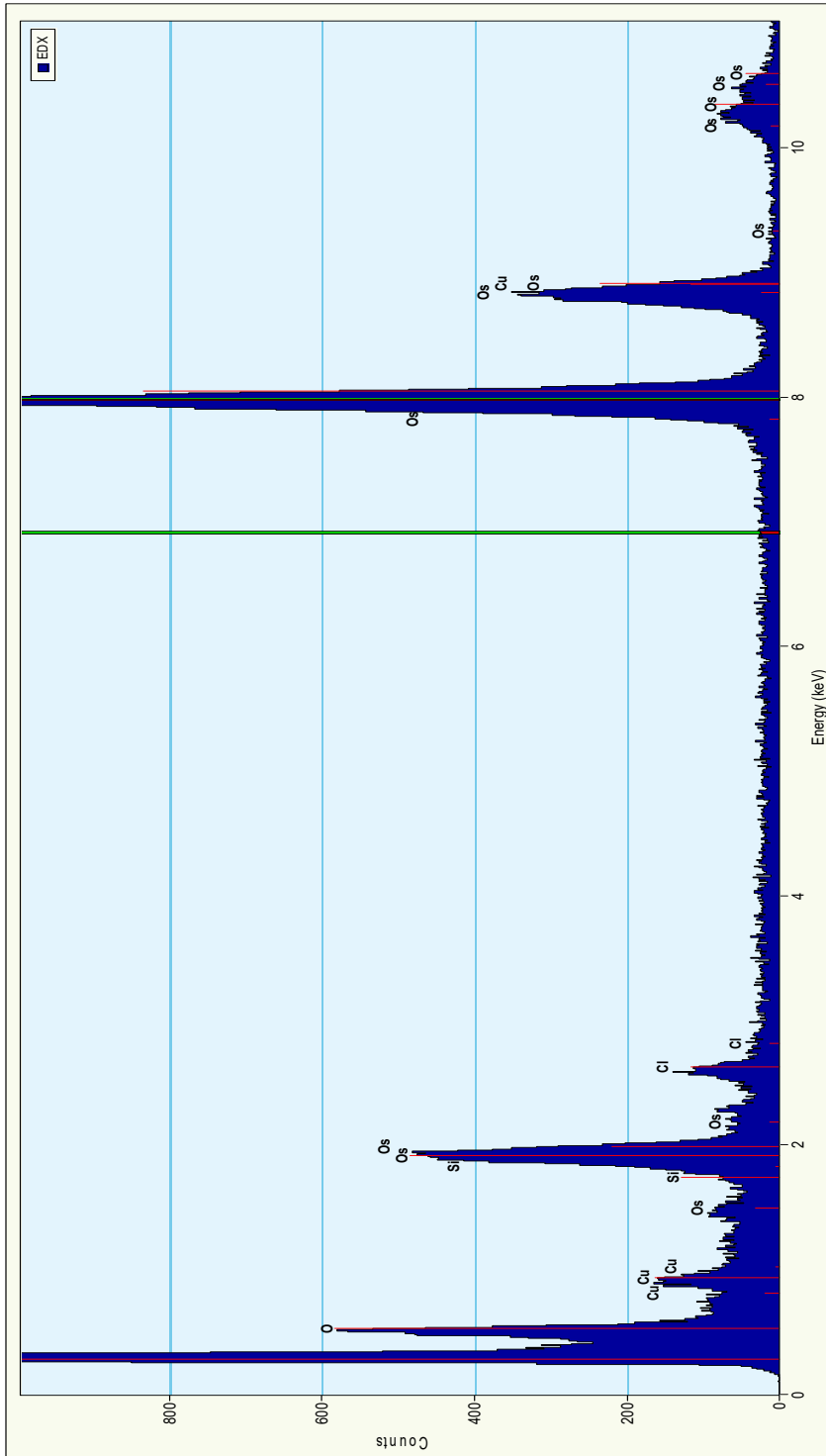


Figure A.1.1. EDS spectra of point 1 from control brain tissue.

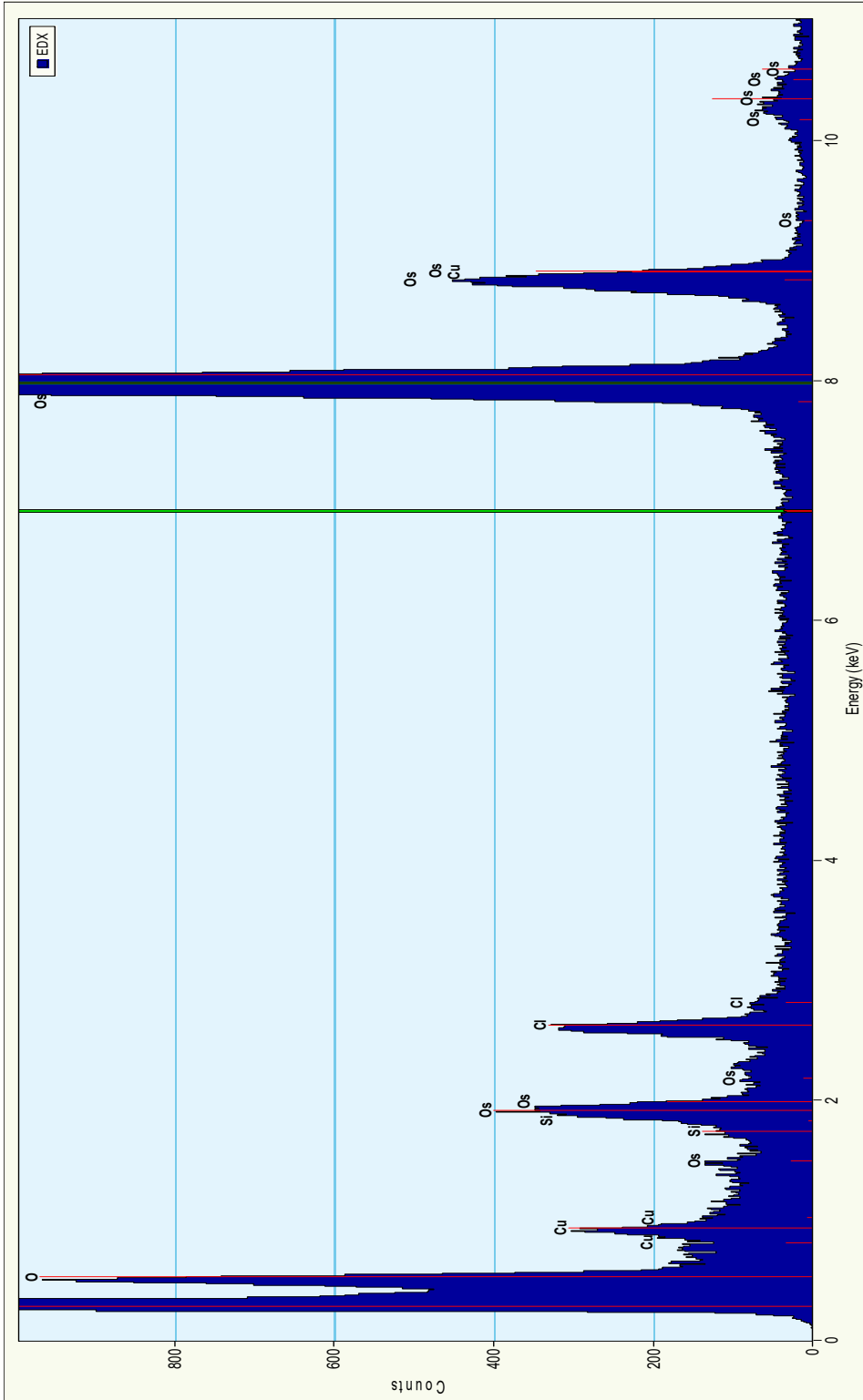


Figure A. 2. EDS spectra of point 2 from control brain tissue.

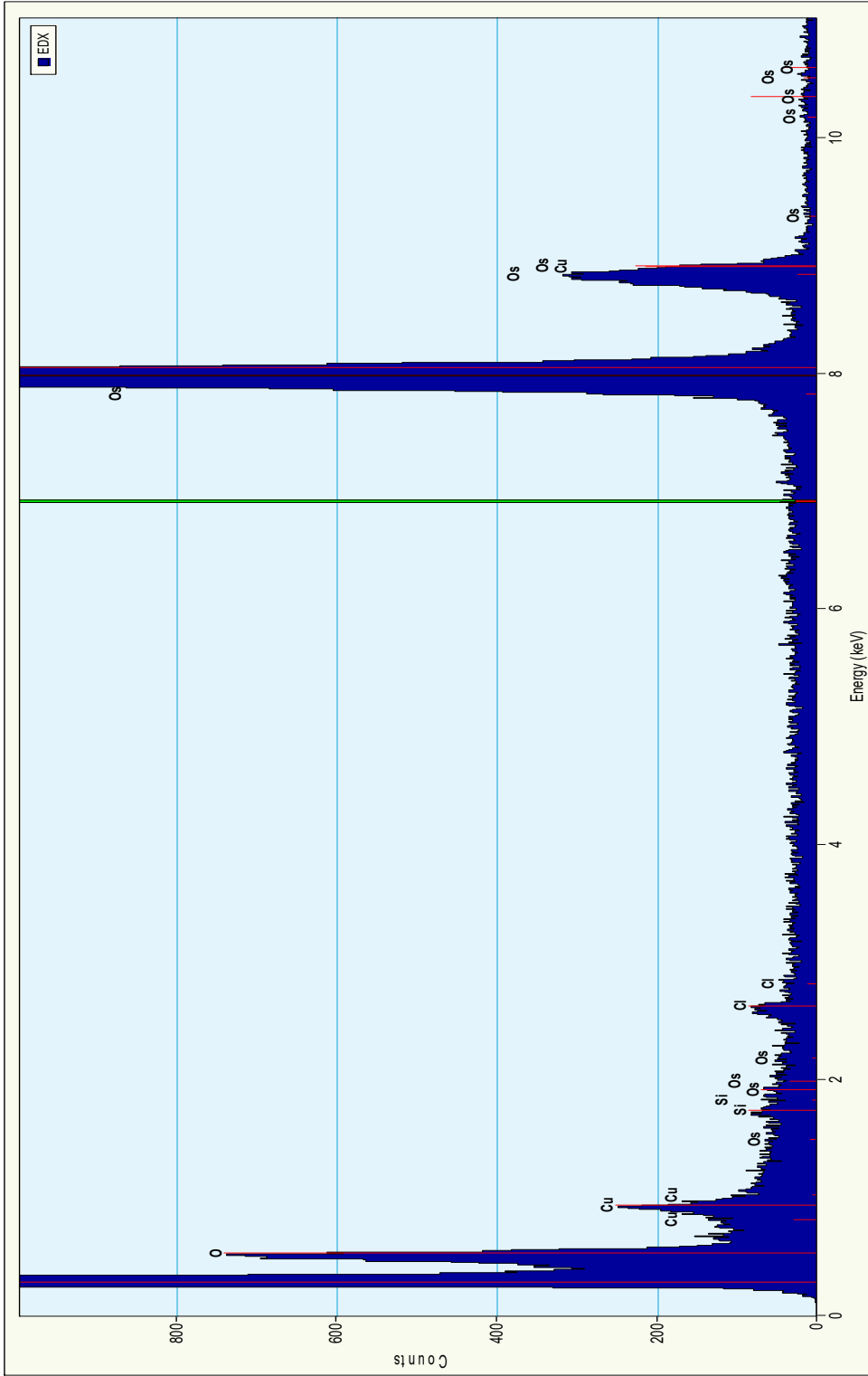


Figure A.3. EDS spectra of point 3 from control brain tissue.

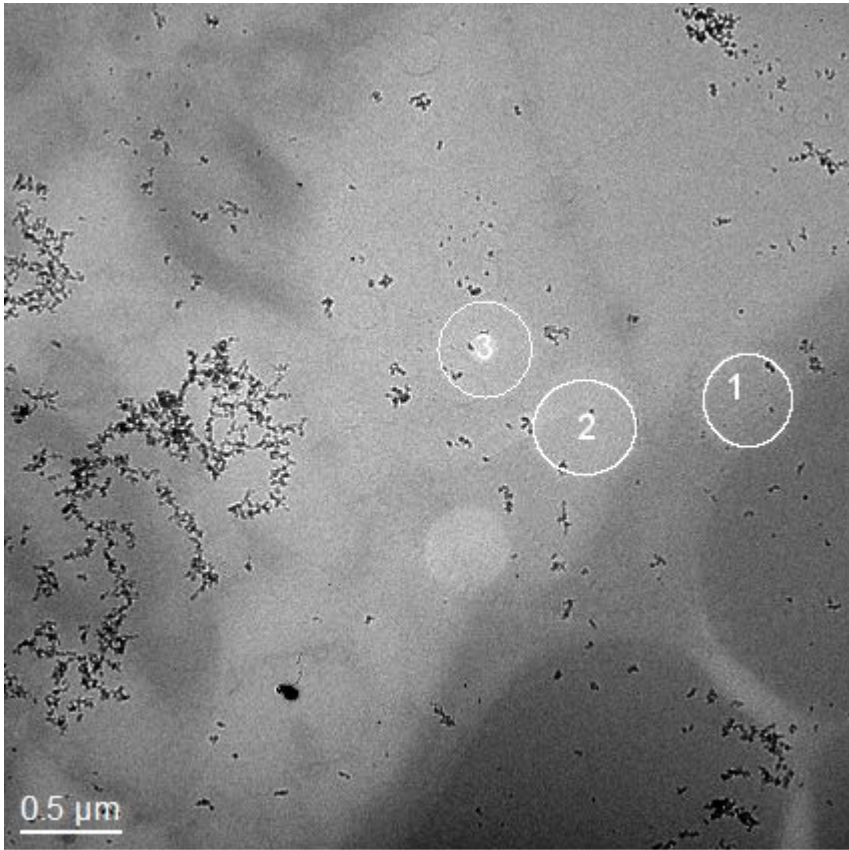


Figure A.4, TEM imaging of soft-PDMS/PDMSO specimen showing sampling points.

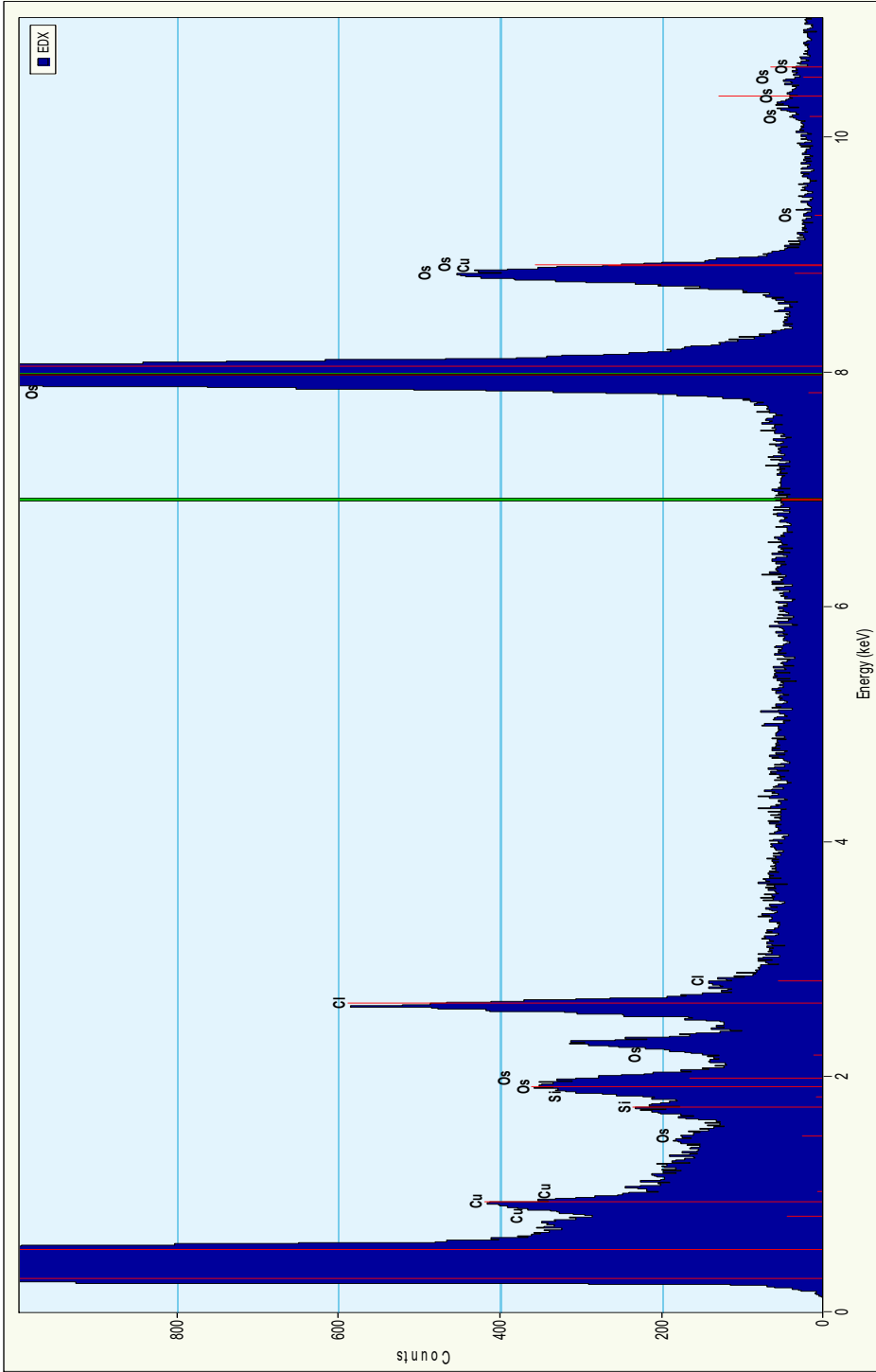


Figure A.5. EDS spectra of point 1 from sample brain tissue.

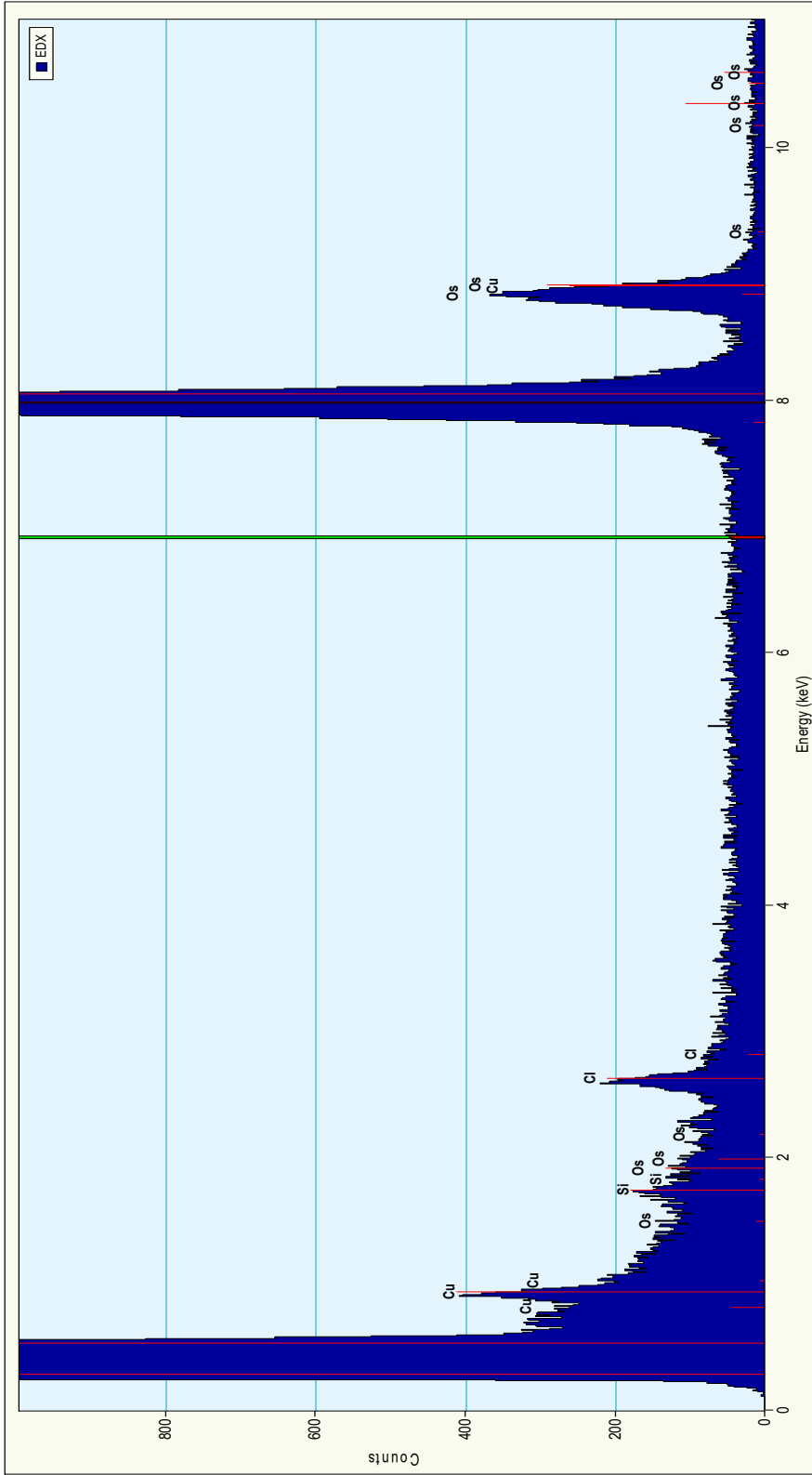


Figure A.6. EDS spectra of point 2 from sample brain tissue.

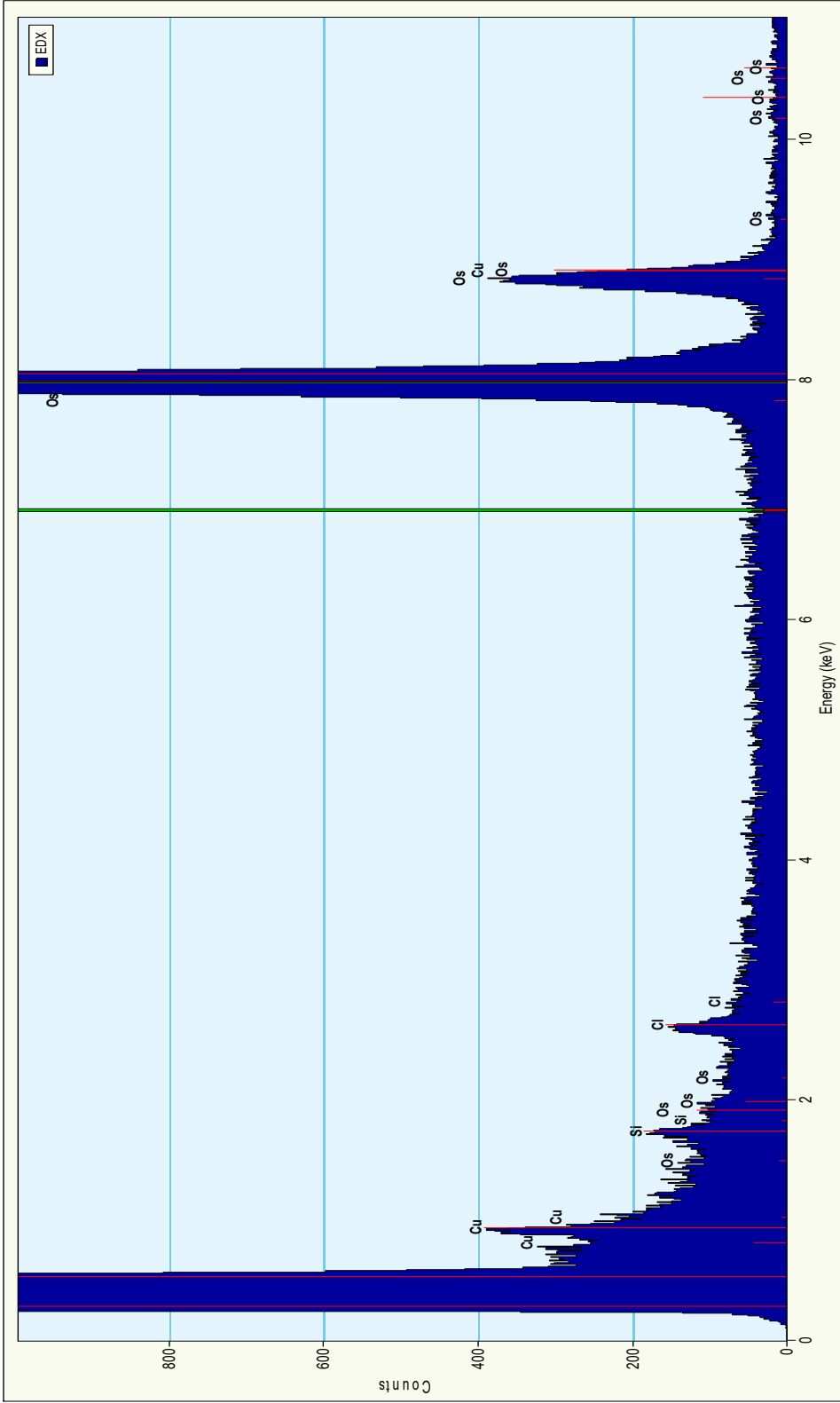


Figure A. 7. EDS spectra of point 3 from sample brain tissue.